10-24-2017

Microperforates: A Review

J Stuart Bolton
Purdue University, bolton@purdue.edu

MICROPERFORATES: A REVIEW

J. Stuart Bolton

Ray W. Herrick Laboratories
Purdue University

LVA / UFSC / KTH Summer School in Aeroacoustics
23 – 26 October 2017

Go to: http://docs.lib.purdue.edu/herrick/ for related presentations

MICROPERFORATED FILMS

Light weight polymer films

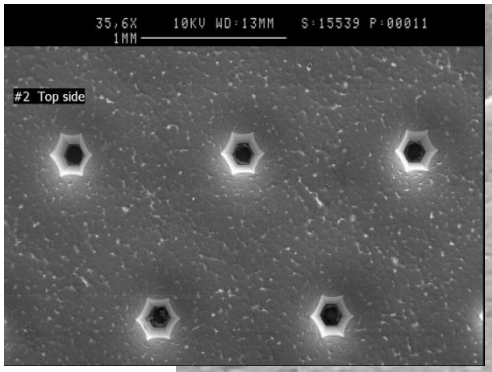

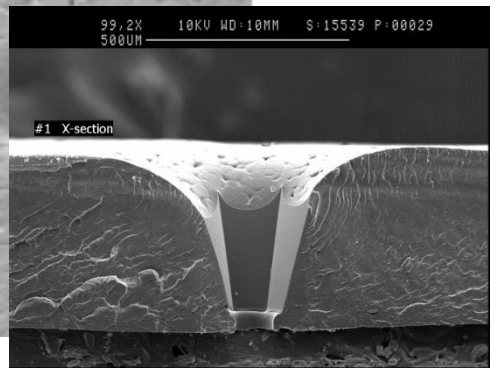

- Hole diameter -- 0.1 mm
- Surface porosity -- 1%

Herrick Labs, Purdue University

INTRODUCTION

- **Microperforated films and sheets**
  - Many attractive functional attributes
    - Fiber free
    - Cleanable
    - Lightweight
    - Printable
    - Easily tunable

MICROPERFORATED FILMS

- **Suggested by Maa in 1975**
  - Cylindrical pore + End corrections
  - Proposed different formulas for thermally conducting and non-conducting boundaries
- **Models needed for design and prediction**
  - Film transfer impedance needed for transmission matrix calculations
  - Need to model non-cylindrical pores
  - Light weight films

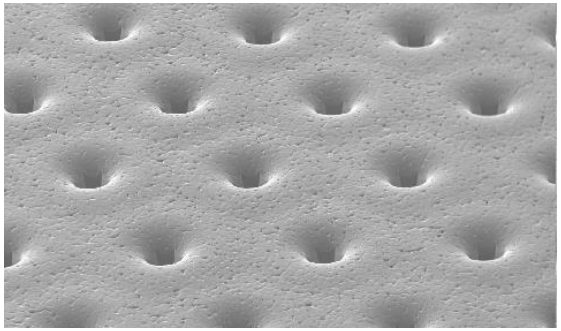

Top view of a microperforated film

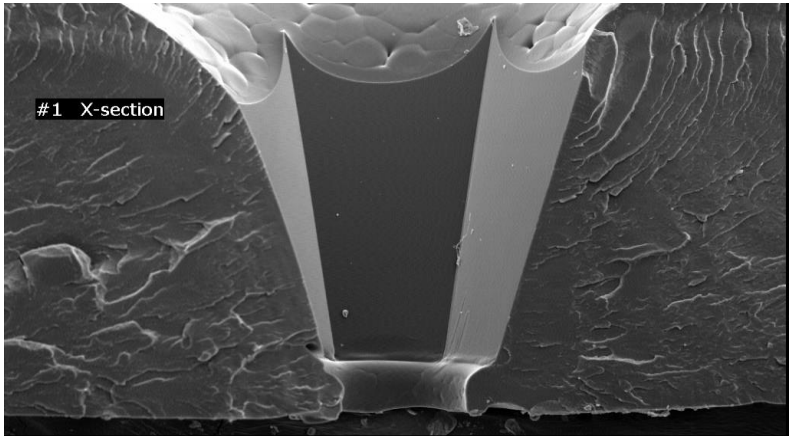

Cross-section of a microperforated film

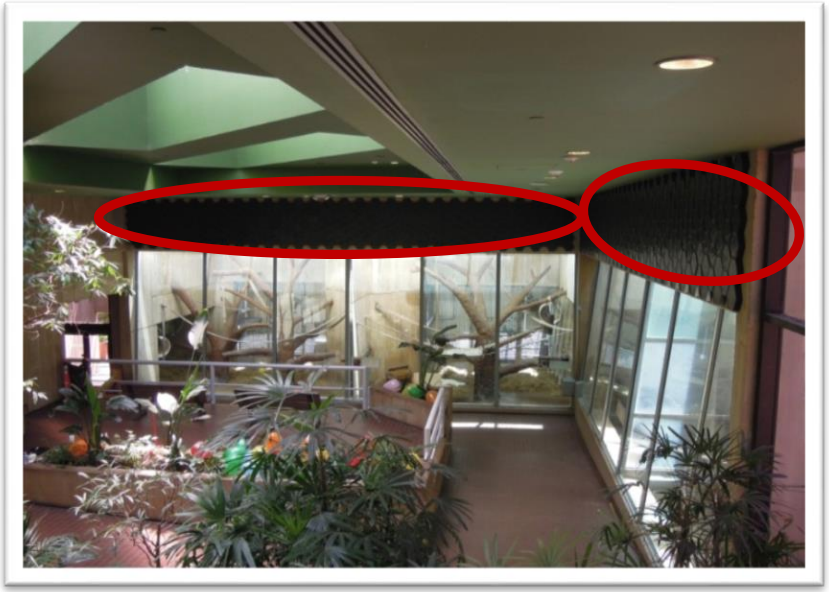

Installed microperforated panels in the Great Ape House of the Smithsonian National Zoo

Herrick Labs, Purdue University

MICROPERFORATED FILMS

- **Perforated Films**

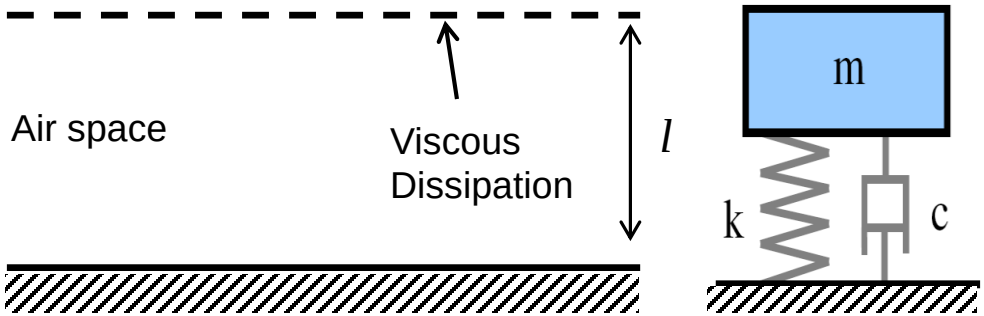

Material Parameters	
• Surface porosity (1%)	• Backing space depth
• Hole size (0.1 mm)	• Hole depth (0.3 mm)

- **Complicating factors**
  - ➢ **Flexibility of the film**
  - ➢ **Non-cylindrical hole shapes**

➢ Owing to low acoustic mass and relatively large viscous losses, absorption bandwidth can be relatively large.

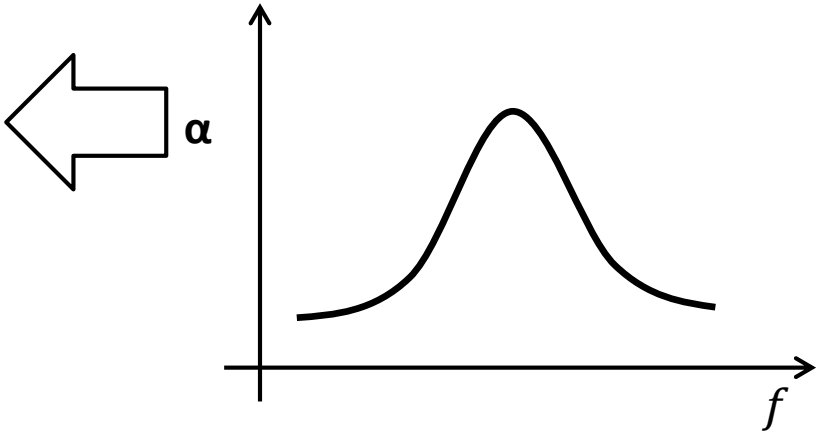

MICROPERFORATED FILMS

- **Tuning:** $Z_n = R - j\rho_0 c\cot(kl)$ **(approximate)**

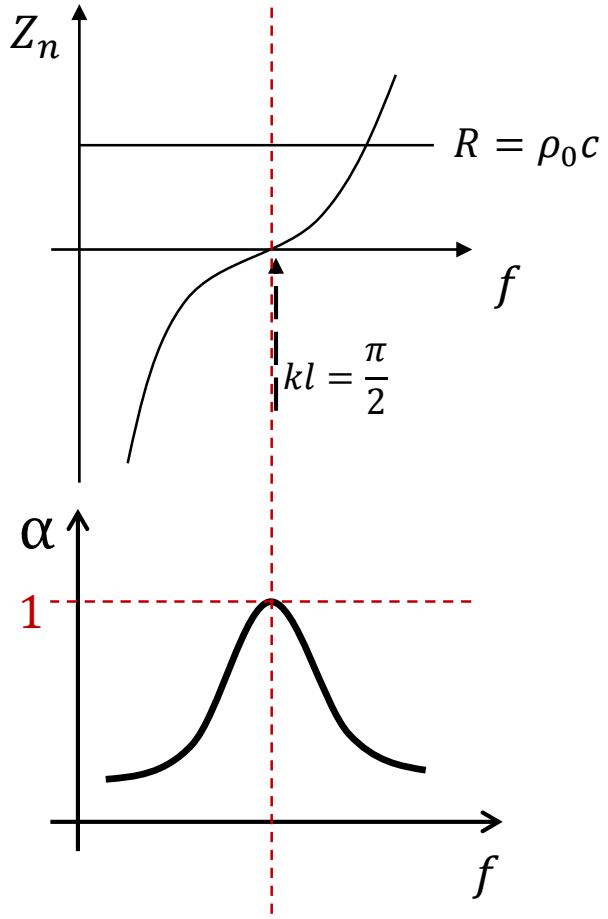

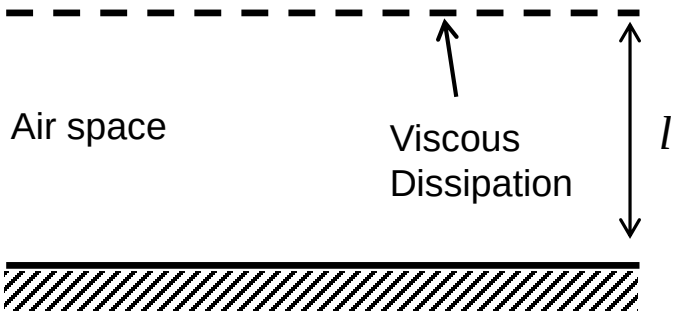

- Peak absorption when imaginary impedance = 0
- Perfect absorption when $R = \rho_0 c$ at that frequency
- Depth of air cavity primarily controls tuning frequency

MICROPERFORATED FILMS

- **Expanding the bandwidth**

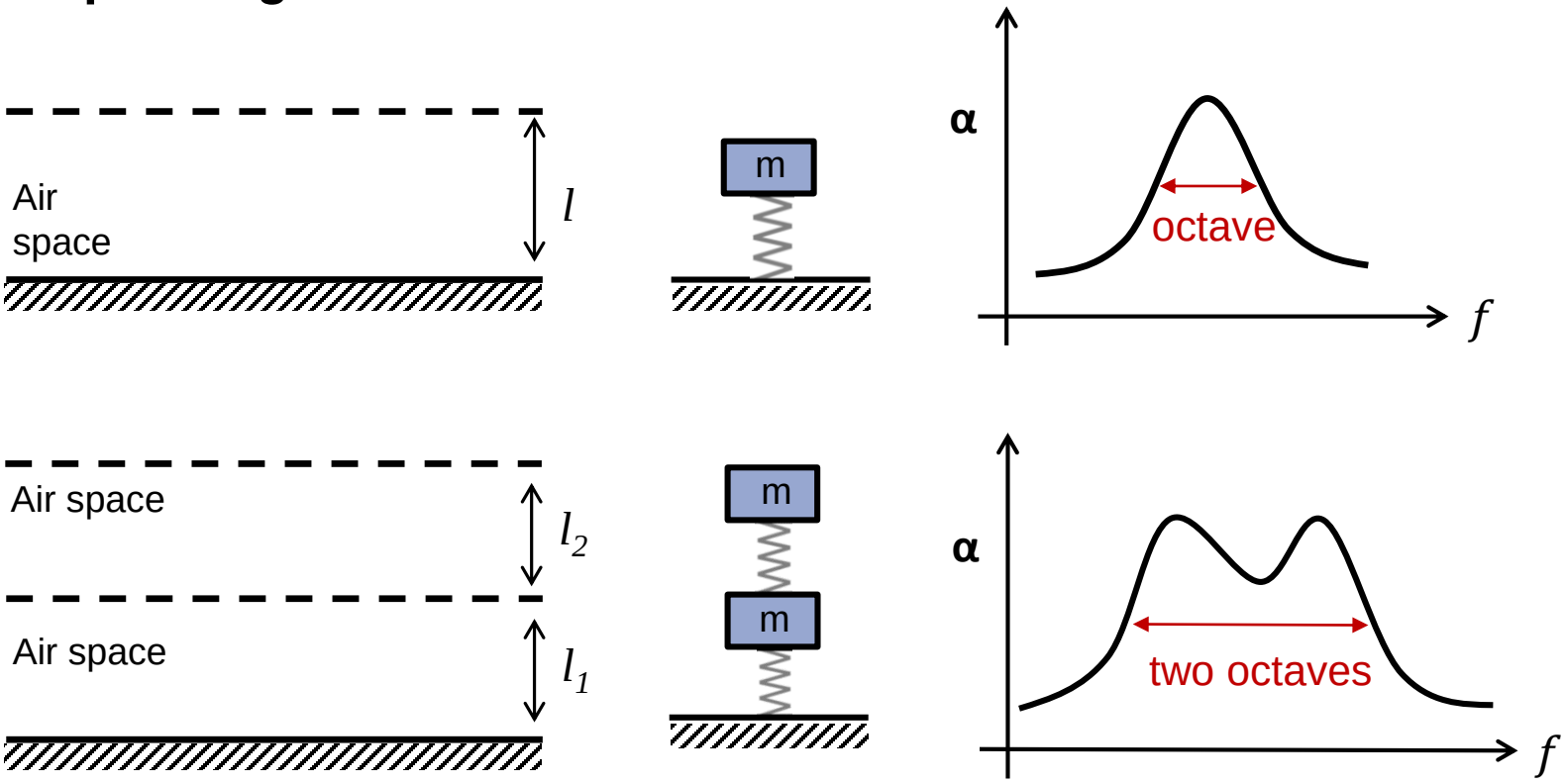

- Expand bandwidth by increasing the degrees of freedom: *i.e.,* add more layers

RANDOM INCIDENCE ABSORPTION MEASUREMENTS

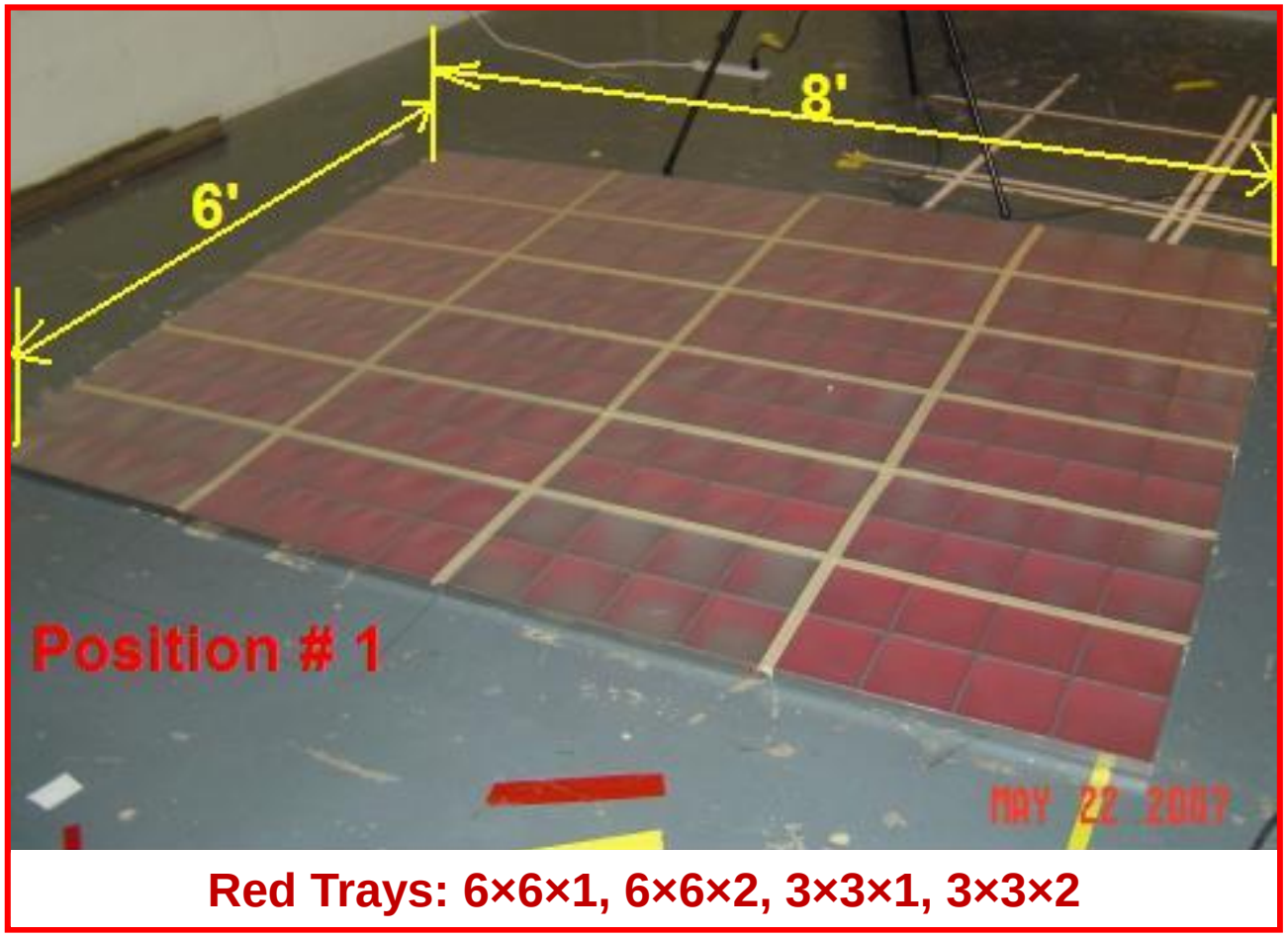

Red Trays: 6×6×1, 6×6×2, 3×3×1, 3×3×2

- Backing trays make air space locally reacting
  - Generally substantial improvement compared to unsegmented air space

RANDOM INCIDENCE ABSORPTION MEASUREMENTS

- **Performance similar to glass fiber or foam in the speech interference range**

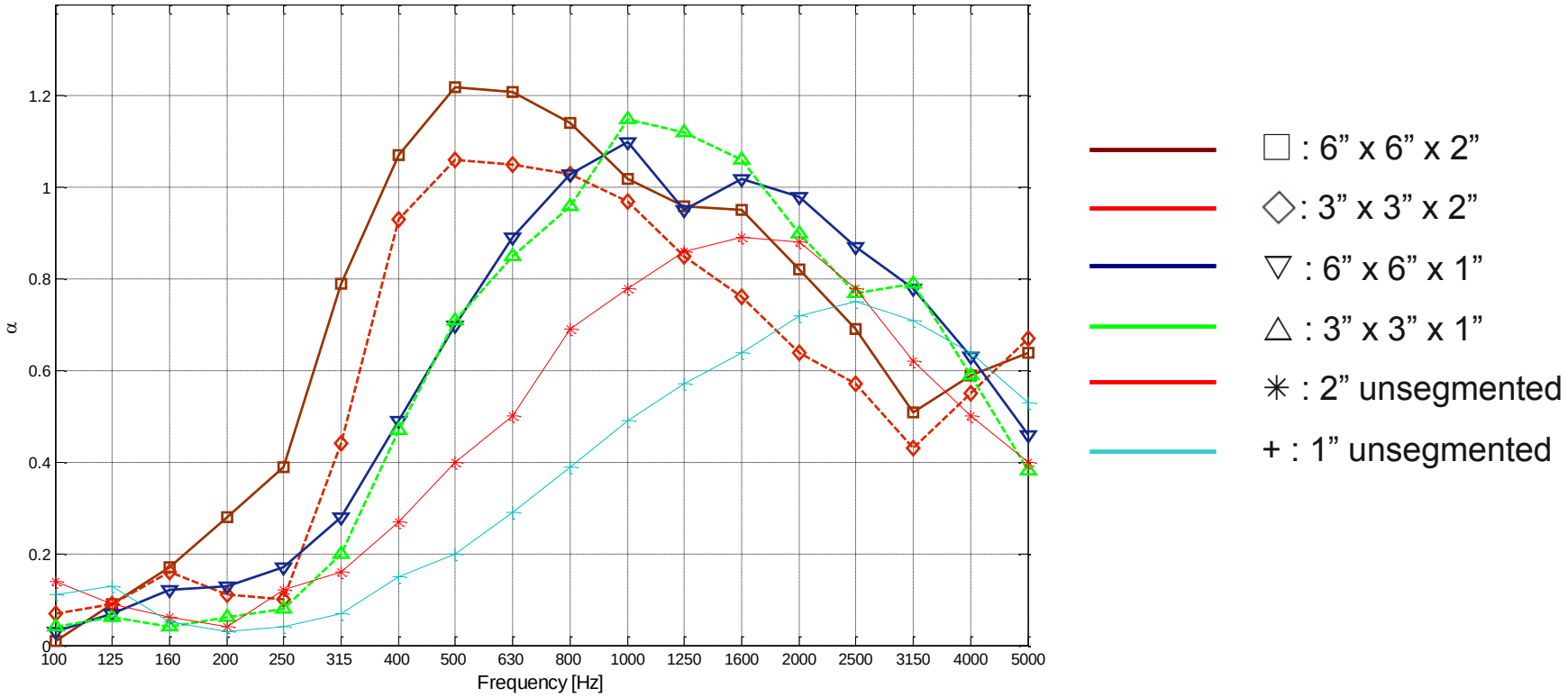

APPLICATIONS

- **Sport facilities**

Herrick Labs, Purdue University

APPLICATIONS

- **Operating rooms**

APPLICATIONS

- **Restaurants**

APPLICATIONS

- **Domestic Interiors**

APPLICATIONS

- National Zoological Park - Great Ape House (Washington DC)

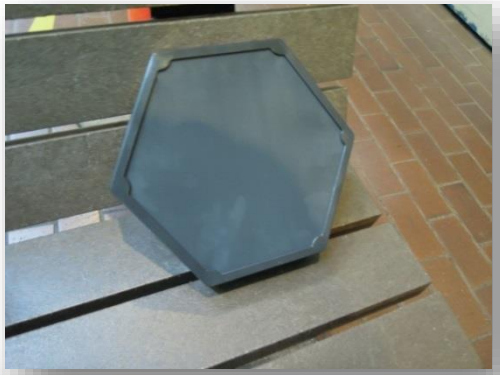

Ryan A. Schultz, J. Stuart Bolton, Jonathan H. Alexander, Stephanie B. Castiglione, Tom P. Hanschen and Ed Bronikowski, "Improving the visitor experience – a noise study and treatment design for the Smithsonian National Zoological Park's Great Ape House," *Proceedings of INTER-NOISE 2012*, 8 pages, 2012.

THE END

(just kidding)

1975 年 1 月　　中　国　科　学　　第 1 期

科学技术成果

微穿孔板吸声结构的理论和设计*

马　大　猷
（中国科学院物理研究所）

摘　　要

薄板上穿以大量的孔，板后留一适当距离，装到墙上，内填多孔性吸声材料，这就形成普通穿孔板吸声结构．它是在环境保护中控制噪声的有效手段，在厅堂音质控制中也可用来改进室内声音的质量．微穿孔板吸声结构是我们在普通穿孔板结构的基础上所作的新发展：把穿孔的直径减小到一毫米以下，而取消板后的多孔性材料，这样不仅大大简化穿孔板结构的构造，并显著地提高它的性能（吸声系数和频率范围）．微穿孔板吸声结构的特点是设计严格，构造简单，成本低，加工简便，并且乎几可以在任何环境下使用．在实践中证明使用效果良好．文中论述了微穿孔板结构的吸声原理和特性，并把结果画成设计图表以简化它的设计步骤，供设计工作者使用．

将此值与准确值(5)式比较，二者符合甚好，最大误差为 6%．（8）式适合于任何 x 值，可代替(6)、(7)二式为更好的近似值．x 当然不能太大，在管中出现横波时，上面的式子就无用了．

管长 t（即穿孔板厚）如果不是比管径 d 大得多，就须要加上末端改正值．声质量的末端改正值是由末端的声辐射而来，使有效管长增加 $0.85d$（计算两端辐射）．声阻的末端改正是由于空气出入微管时有一部分沿障板流动，因而产生磨擦损失所致．因此可求得[7]，两端外都是无穷平面障板时，声阻率增加 $2\sqrt{2\omega\rho\eta}$．这两部分都应加于（8）式．

微穿孔板的声阻抗率，如果假设各孔间互不影响，就等于单管的声阻抗率(包括末端改正值）除以穿孔率 p（每单位板面积上孔的总面积）．以空气的特性声阻 ρc（c 为声速）为单位，穿孔板的相对声阻抗就等于：

$$z = \frac{Z_1}{p\rho c} = r + j\omega m, \tag{9}$$

其中相对声阻和相对声质量分别为：

$$r = \frac{32\mu}{pc}\frac{t}{d^2}\left[\sqrt{1+\frac{x^2}{32}} + \frac{\sqrt{2}\,x}{8}\frac{d}{t}\right], \tag{10}$$

Vol. XVIII No. 1 SCIENTIA SINICA Jan.-Feb. 1975

THEORY AND DESIGN OF MICROPERFORATED PANEL SOUND-ABSORBING CONSTRUCTIONS

MAA DAH-YOU (马大猷)

(*Institute of Physics, Academia Sinica*)

Received May 2, 1974.

ABSTRACT

Theory and design of perforated panel sound-absorbing constructions are well developed, but the difficulties in adjusting the acoustic resistance part of such constructions curtail their usefulness. In this paper, a revolutionary idea is proposed that the perforations are to be reduced to submillimetre level so that they themselves will provide sufficient acoustic resistance while the low acoustic mass is retained, and so the difficulty of acoustic resistances is resolved. Practice shows that this idea is correct. Such panels are now named microperforated panels. Their features are predictable absorption characteristics, simple structures and in addition, wide frequency bands of absorption. The elimination of porous materials makes the microperforated panel constructions windproof and waterproof, and also heatproof and even flameproof for short time if they are fabricated with sheet metal or other fireproof materials. Therefore, the problem of wide band, high coefficient sound absorber for severe circumstances is solved for good. Acoustical properties and unified formulae for perforations of all sizes are derived; the theory and characteristics of the microperforated panel constructions as well as design charts are given to facilitate the practical design work. Ordinary perforated panel constructions are given as a special case.

and compare with the exact values, they agree well, the error being no more than 6%. Eq. (8), as a better approximation of Eq. (5) than Eqs. (6) and (7), is valid for any value of x, up to the value where transversal modes begin to appear in the tube.

End corrections must be added, unless the tube length t (i. e., the thickness of the panel) is large compared with the tube diameter d, Rayleigh[4] showed that the end correction of the acoustic mass comes from the sound radiation from the ends of the tube, and makes the effective length of the tube increased by 0.85 d if radiation from both ends are counted. End correction of the acoustic resistance is produced by the friction loss due to a part of the air moves along the baffle when the air flows into and out of the tube, and it may be found[7] that the additional part of the acoustic resistance is $2\sqrt{2\omega\rho\eta}$, if both sides of the tube are ended in infinite baffles.

The specific acoustic impedance of the microperforated panel is equal to the specific acoustic impedance of a single tube (plus end corrections) divided by the percentage perforation p (total area of the perforation on a unit area of panel), provided that the interference between the pores can be neglected. In unit of the characteristic impedance of air, ρc (c being the velocity of sound), the relative acoustic impedance is

$$z = \frac{Z_1}{p\rho c} = r + j\omega m, \tag{9}$$

End correction of the acoustic resistance is produced by the friction loss due to a part of the air moves along the baffle when the air flows into and out of the tube, and it may be found[7] that the additional part of the acoustic resistance is $2\sqrt{2\omega\rho\eta}$, if both sides of the tube are ended in infinite baffles.

THE JOURNAL
OF THE
ACOUSTICAL SOCIETY OF AMERICA

Volume 25 Number 6

NOVEMBER • 1953

On the Theory and Design of Acoustic Resonators*†

UNO INGARD
Acoustics Laboratory, Massachusetts Institute of Technology, Cambridge, Massachusetts
(Received June 19, 1953)

Absorption and scattering from resonators in a free field as well as in walls are discussed. The effect of different aperture geometries on the resonance frequency of resonators is considered and illustrated by examples. Considering losses due to viscosity, heat conduction, and radiation, the optimum design for maximum resonance absorption is analyzed, and the results are expressed in terms of design charts. Nonlinear effects on the absorption and resonance frequency are also included, and a discussion of the onset of turbulence is presented.

Effect of Viscosity

The dissipation caused by viscosity can be calculated approximately from the integral[9]

$$W_v = \frac{1}{2}\int_S R_S |U_S|^2 dS, \tag{8}$$

where U_S is the tangential velocity amplitude at the surface S calculated from the wave equation neglecting viscosity, and R_S is a "surface resistance." If the radius of curvature of the surface under consideration is large compared to the viscous boundary layer thickness, one can as a good approximation use the resistance calculated from the problem of an oscillatory flow over an infinite plane surface. This resistance is[10]

$$R_S = \tfrac{1}{2}(2\mu\rho\omega)^{\frac{1}{2}}, \tag{9}$$

where μ is the viscosity and ρ the density of the medium. At ordinary room tempertaure, $t \simeq 20°C$, the numerical value for the surface resistance becomes

$$R_S \simeq 0.83 \cdot 10^{-3}(\nu)^{\frac{1}{2}}, \tag{10}$$

where ν is the frequency.

TABLE III. Measurements of end correction.

Diameter $2r_0$ cm	Measured slope S of curves in Fig. 9	Total equivalent neck length l cm	Neck length t cm	End correction $2\delta = l - t$	2δ calculated
0.36	$0.406\ 10^{-3}$	0.390	0.097	0.283	0.284
0.50	$0.324\ 10^{-3}$	0.430	0.051	0.379	0.387
1.00	$0.276\ 10^{-3}$	0.736	0.051	0.685	0.707
1.40	$0.245\ 10^{-3}$	0.920	0.051	0.869	0.890
2.00	$0.207\ 10^{-3}$	1.110	0.051	1.059	1.12

MAA MODEL (1975) - CYLINDRICAL

$$z = \frac{Z_1}{\sigma \rho_0 c} = r + j\omega m$$

- Z_1: specific acoustic impedance of single hole
- σ: porosity
- r: resistance
- m: effective mass per unit area

- Perforation constant $x = 210d\sqrt{f}$ Related to boundary layer

d: hole diameter
f: frequency
t: hole depth
c: speed of sound
μ: kinematic viscosity
v: thermal conductivity
L: backing depth

- Resistance $r = \frac{32(\mu + v)}{\sigma c}\frac{t}{d^2}\left(\sqrt{1+\frac{x^2}{32}} + \frac{\sqrt{2}}{8}x\frac{d}{t}\right)$

Contribution from hole

End corrections (effect from flow over outer surface and convergence into and out of holes)

- Reactance $m = \frac{t}{\sigma c}\left(1 + \frac{1}{\sqrt{9+\frac{x^2}{2}}} + 0.85\frac{d}{t}\right)$

- Absorption Coefficient $\alpha_n = \frac{4r}{(1+r)^2 + \left(\omega m - \cot\left(\frac{\omega L}{c}\right)\right)^2}$

Panel is assumed RIGID in Maa models: no flexural motion is considered

MAA MODELS

Substantial change in Resistance

Not much change in Reactance

Models	Perforation constant	Resistance	Reactance
1975 High thermal conductivity model- Scientia Sinica	$x = 210d\sqrt{f}$	$r = \frac{32(\mu+v)}{\sigma c}\frac{t}{d^2}\left(\sqrt{1+\frac{x^2}{32}}+\frac{\sqrt{2}}{8}x\frac{d}{t}\right)$	$m = \frac{t}{\sigma c}\left(1+\frac{1}{\sqrt{9+\frac{x^2}{2}}}+0.85\frac{d}{t}\right)$
1975 Low thermal conductivity model- Scientia Sinica	$x = 316d\sqrt{f}$	$r = \frac{32\mu}{\sigma c}\frac{t}{d^2}\left(\sqrt{1+\frac{x^2}{32}}+\frac{\sqrt{2}}{8}x\frac{d}{t}\right)$	$m = \frac{t}{\sigma c}\left(1+\frac{1}{\sqrt{9+\frac{x^2}{2}}}+0.85\frac{d}{t}\right)$
1987 Noise Control Engineering Journal	$x = d\sqrt{\frac{\omega\rho_0}{4\eta}}$	$r = \frac{32\eta}{\sigma\rho_0 c}\frac{t}{d^2}\left(\sqrt{1+\frac{x^2}{32}}+\sqrt{\frac{2xd}{8t}}\right)$	$m = \frac{t}{\sigma c}\left(1+\frac{1}{\sqrt{9+\frac{x^2}{2}}}+0.85\frac{d}{t}\right)$
1998 Journal of Acoustical Society of America	$x = d\sqrt{\frac{\omega\rho_0}{4\eta}}$	$r = \frac{32\eta}{\sigma\rho_0 c}\frac{t}{d^2}\left(\sqrt{1+\frac{x^2}{32}}+\frac{\sqrt{2}}{32}x\frac{d}{t}\right)$	$m = \frac{t}{\sigma c}\left(1+\frac{1}{\sqrt{1+\frac{x^2}{2}}}+0.85\frac{d}{t}\right)$

- d: hole diameter, f: frequency, t: hole depth, c: speed of sound, μ: kinematic viscosity, v: thermal conductivity, η: viscosity coefficient ($=\mu\rho_0$)

BRASS SAMPLES

Sample number	Hole diameter *d* [mm]	Hole depth *t* [mm]	Number of holes per m^2	*t/d*	Mass/area [kg/m^2]	Porosity [%]
2	0.185	1.27	6.20×10^5	6.8	9.8	1.7
3	0.41	0.406	3.03×10^5	1	3.2	4
4	0.413	0.813	6.07×10^5	2	5.9	8.1

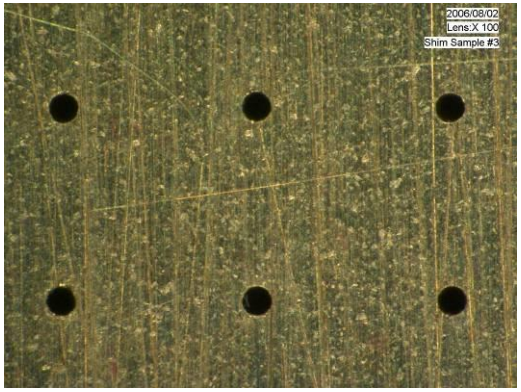

Sample 2 (x100)

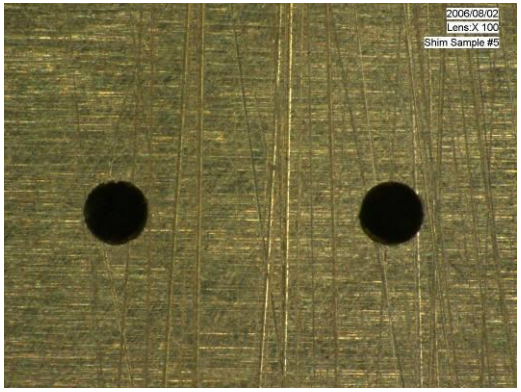

Sample 3 (x100)

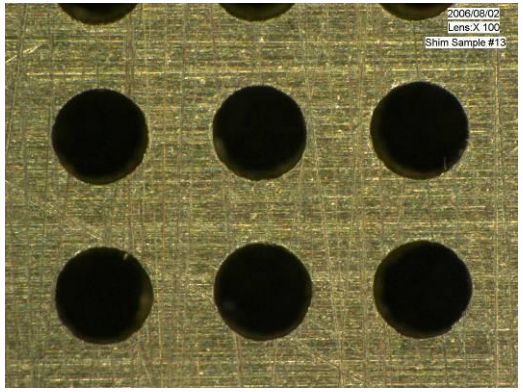

Sample 10 (x100)

MEASUREMENTS AND PREDICTIONS FROM VARIOUS MAA MODELS

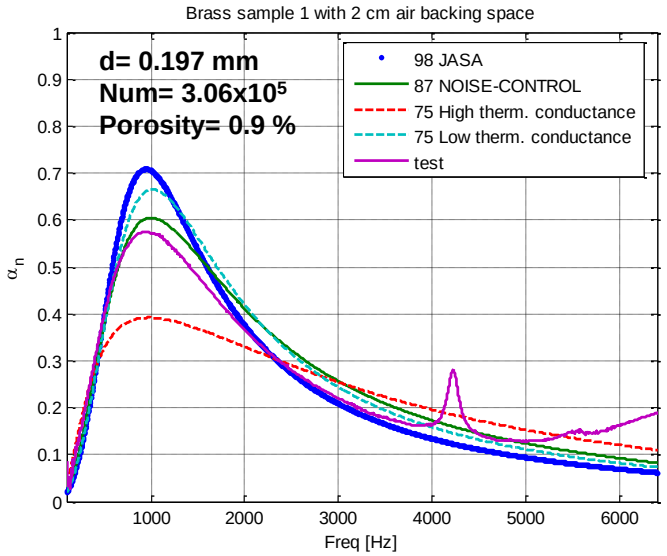

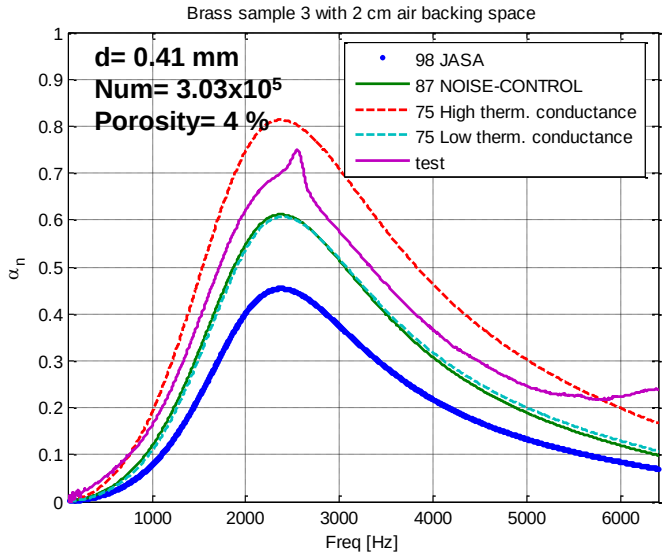

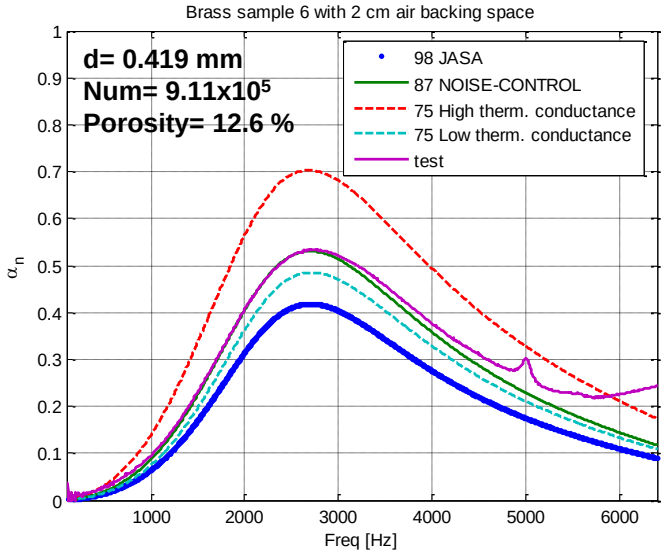

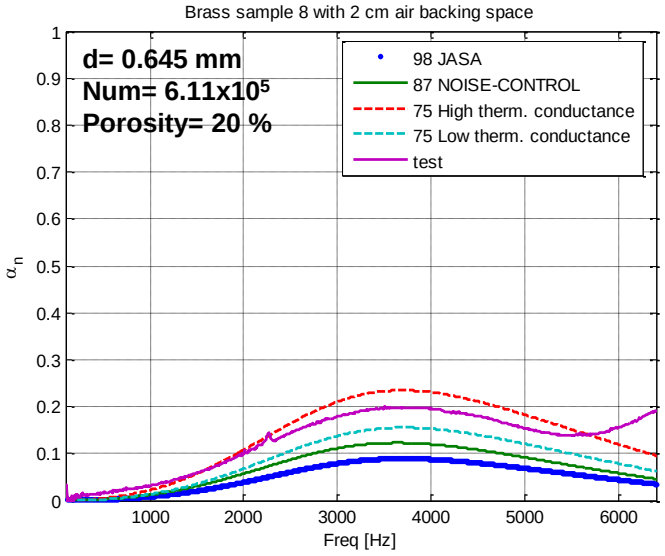

- There are significant differences on absorption predictions depending on model used
- Which one gives the most accurate prediction?
- 87 NCEJ?

Herrick Labs, Purdue University

MODEL PERFORMANCE

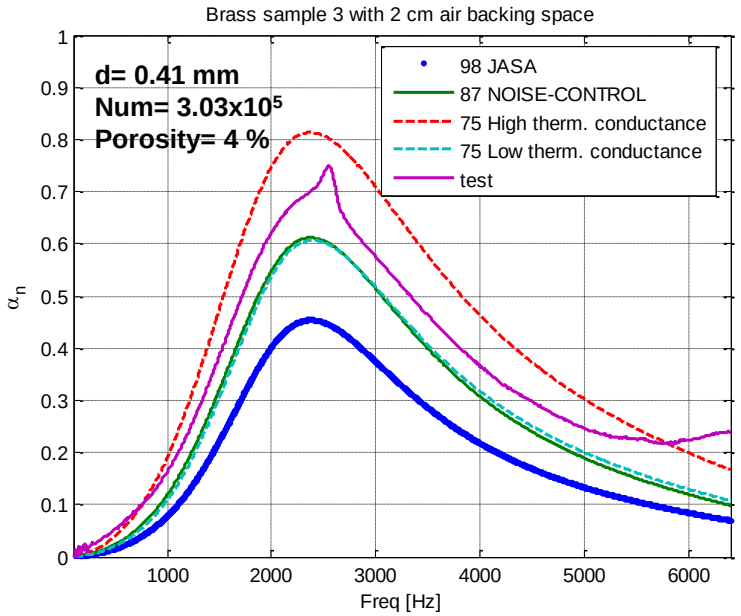

- **Observations**
  - Absorption peak locations accurately predicted in all cases- reactive part of model impedance is assumed to be accurate
  - Absorption peaks heights are not predicted accurately consistently by any of the models – so, resistive end correction is assumed to be inaccurate

TRANSFER IMPEDANCE OF MICROPERFORATED FILMS – COMPLICATIONS

- Resistive end corrections
- Arbitrarily–shaped holes
- Thermal effects
- Fluid-structure interaction

CFD APPROACH
– INSPIRED BY C. K. W. TAM*

- Objective

  By using computational fluid dynamics approach, calculate dynamic flow resistance for microperforated panel considering flow through one hole and compare with existing formulation

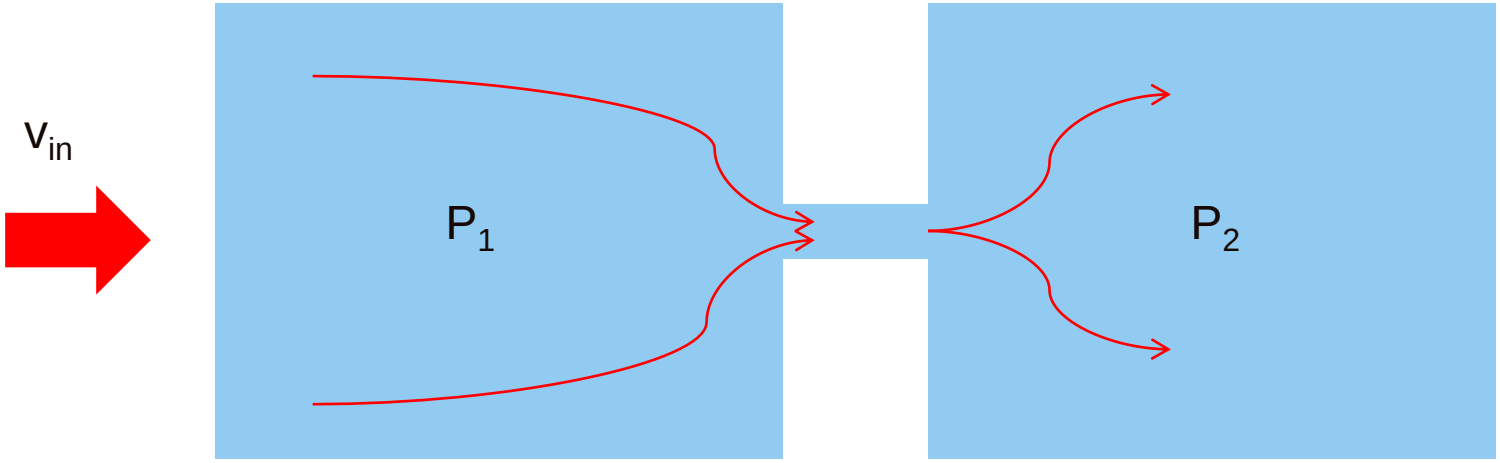

$$R_f = \frac{P_1 - P_2}{v_{in}}$$

*C. K. W. Tam, H. Ju, M. G. Jones, W. R. Watson and T. L. Parrott, "A computational and experimental study of slit resonators." *Journal of Sound and Vibration*, June 2005, Vol. 284, Issues 3-5, p. 947–984

GEOMETRY AND ASSUMPTIONS

- Geometry of CFD model

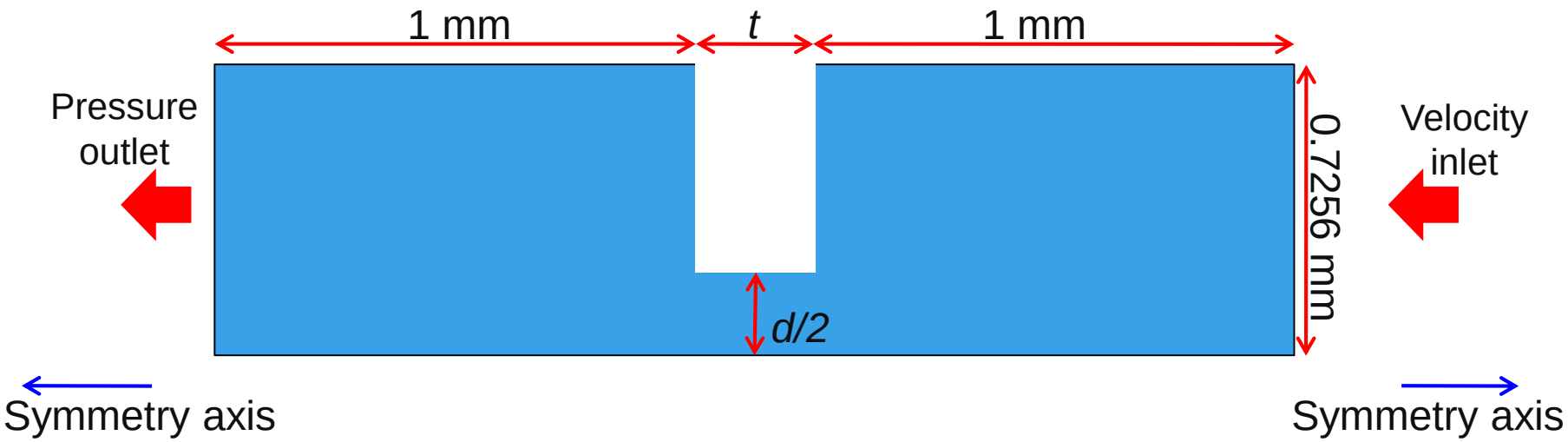

- Incompressible flow in Fluent
- Mesh Interval : 0.005 mm, pressure-based, implicit formulation
- the Green-Gauss node-based method
- SIMPLE for the pressure-velocity coupling method
- STANDARD for pressure
- SECOND-ORDER UPWIND for momentum

INLET VELOCITY AND PRESSURE

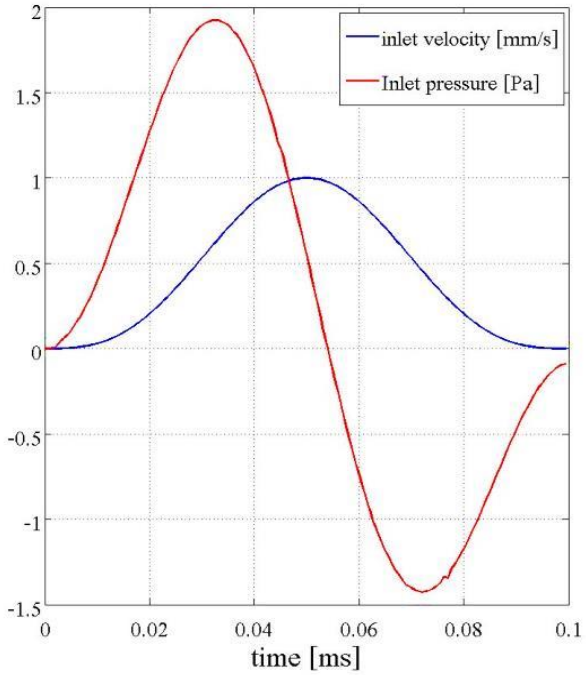

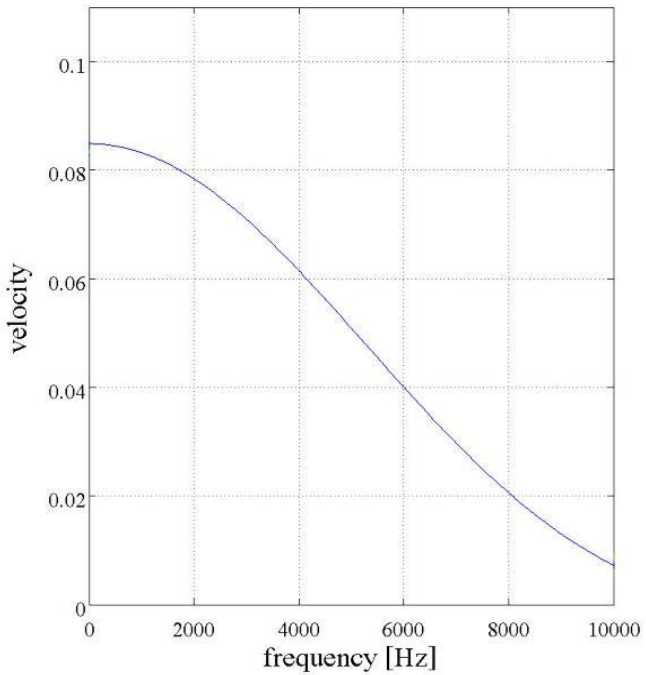

- Inlet velocity was chosen to be a Hann windowed, 5 kHz half-sine wave having a maximum value of 1 mm/s in order to cover the frequency range up to 10 kHz

MAA MODEL*

Cylinder Surface

$$R = \left(Re\left\{ \frac{j\omega t}{\sigma c}\left[1 - \frac{2}{k\sqrt{-j}} \frac{J_1\left(k\sqrt{-j}\right)}{J_0\left(k\sqrt{-j}\right)} \right]^{-1} \right\} + \frac{\alpha 2 R_s}{\sigma \rho c} \right) \times \rho c$$

$$k = d\sqrt{\frac{\omega \rho_0}{4\eta}}$$

$\alpha = 2$ when smooth end

$$R_s = \frac{\sqrt{2\omega\rho_0\eta}}{2}$$

$\alpha = 4$ when sharp end

➡ **Dynamic flow resistance (R) is function of *t*, *d*, *σ***

➡ **Note that $R_s \rightarrow 0$ as $\omega \rightarrow 0$**

*Y. Guo, S. Allam and M. Abom. “Micro-perforated plates for vehicle applications.” *Proceedings of INTER-NOISE 2008*, Shanghai, China, 2008.

COMPARISON OF CFD WITH MAA MODEL

- Dynamic flow resistance and flow reactance (*d*=0.4064 mm, *t*=0.4064 mm, *σ*=0.02)

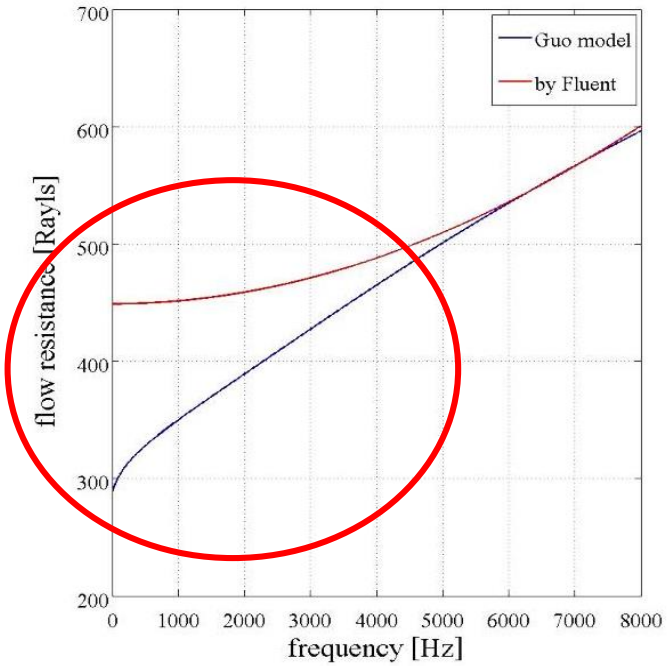

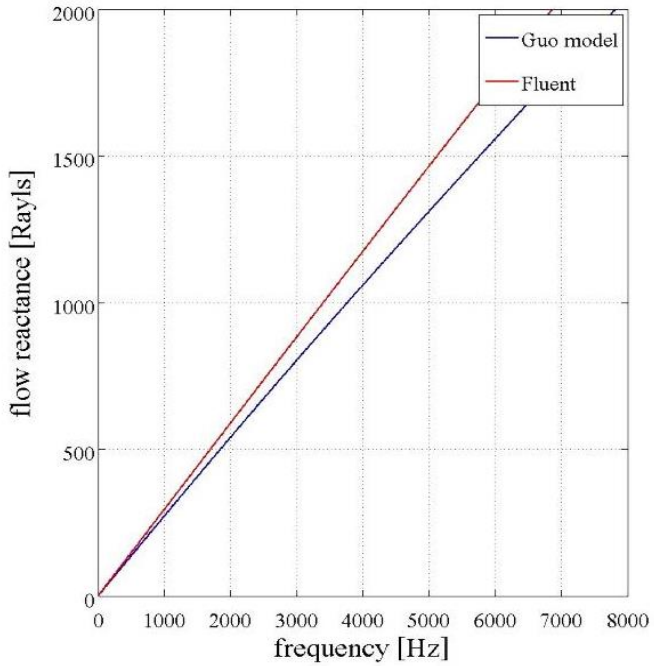

Large difference in flow Resistance in low frequency range

Make *α,* which is defined by Guo *et al.,* a function of frequency to fit with CFD results

RIGID FILM – VISCOUS LOSSES

$$\langle E_{loss} \rangle_{\mu} = \mu \langle |\nabla u|^2 \rangle$$

- **Viscous energy losses are proportional to the shear rate squared**
  - Losses are concentrated along perforation walls and at the inlet/outlet *(resistive end correction)*
  - Losses are symmetric front-to-back in linear regime *(acoustic wave is incident from below)*
  - Losses decrease as the frequency increases

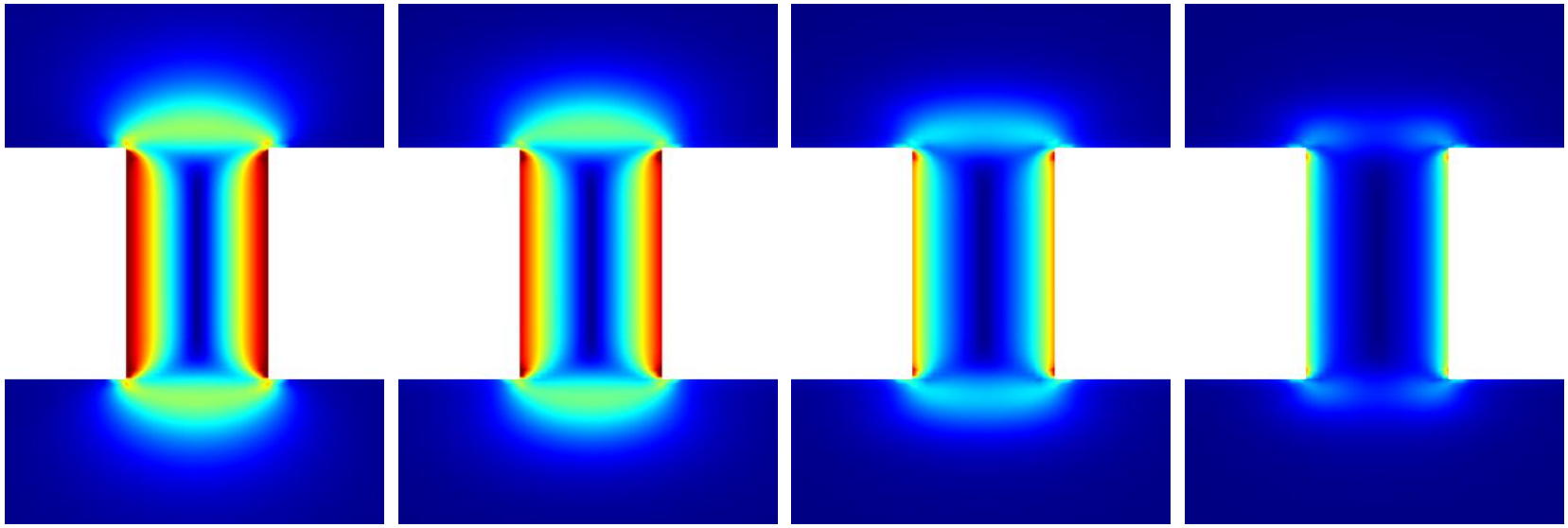

500 Hz **2,000 Hz** **5,000 Hz** **10,000 Hz**

Plots of the square root of viscous losses on a scale from 0 to 15 $\sqrt{W/m^3}$

RESISTIVE END CORRECTION

- Energy dissipation occurs within shearing fluid external to the hole – not on the solid surface adjacent to the holes
- Net result is that the resistive end correction is independent of frequency (*unlike Maa* $\propto \omega^{1/2}$)
- Resistive end correction remains finite at zero Hz

CFD MODEL – CONICAL HOLES

- **Axisymmetric tapered holes shape**
- **FE code Comsol was used primarily**

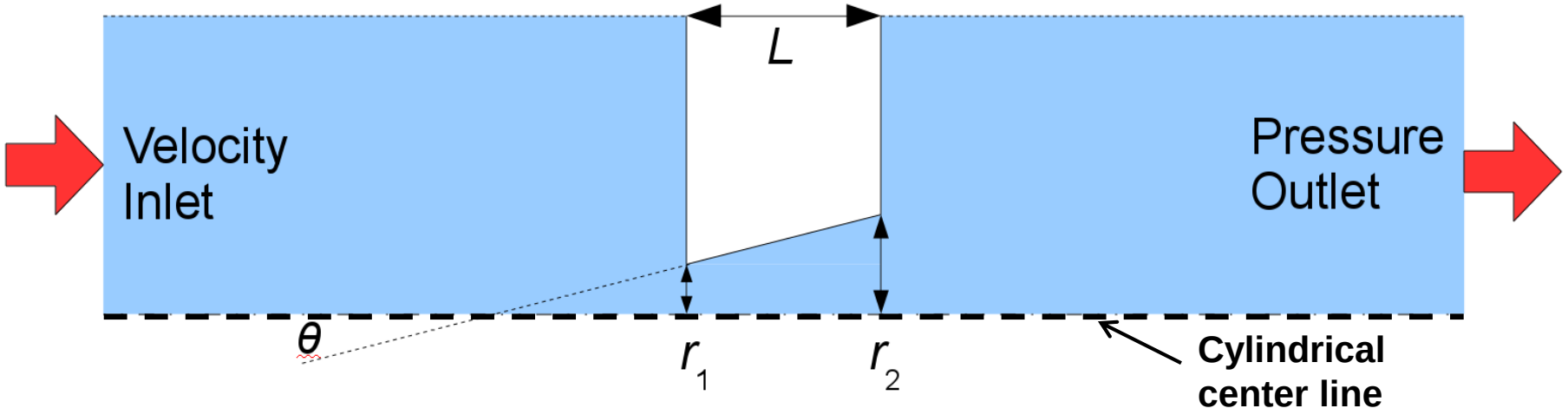

- Incompressible, isothermal, 2D axisymmetric
- Inlet: Hann-windowed, 5 kHz half-sine (0.1 ms) - velocity
- Run 0.5 ms for accurate static flow resistance
- Maximum speed of 1 mm/s
- **Represents infinite square array**

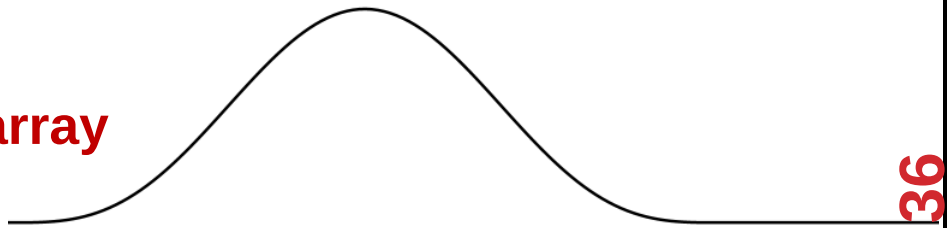

COMPARISON WITH SAKAGAMI CASE

- A pilot study on improving the absorptivity of a thick microperforated panel absorber, Sakagami *et al.*

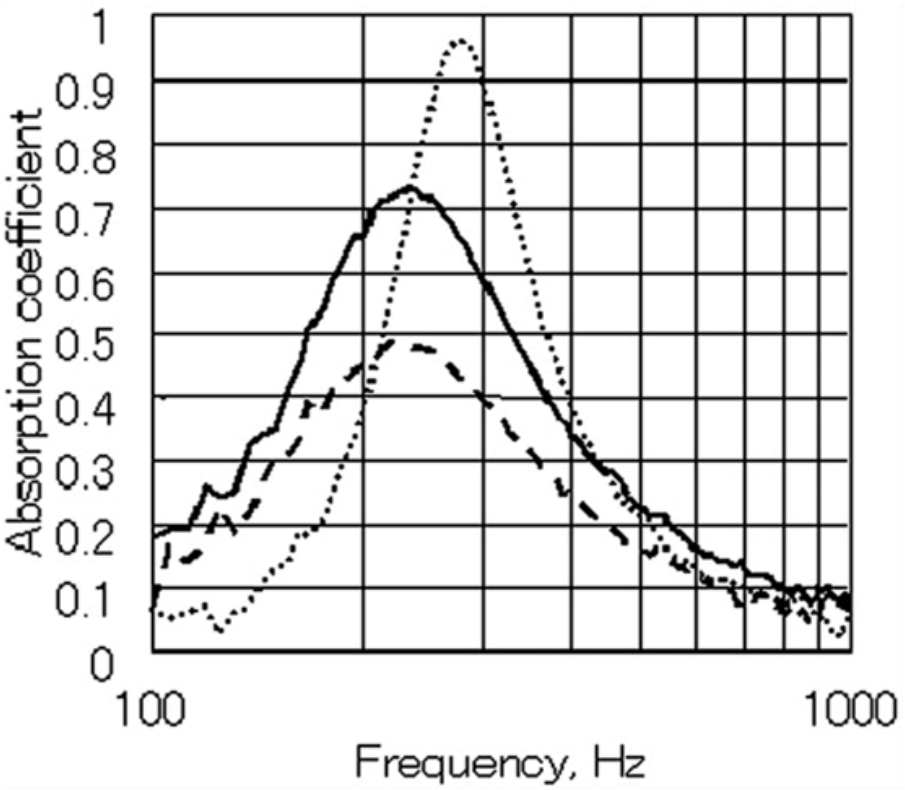

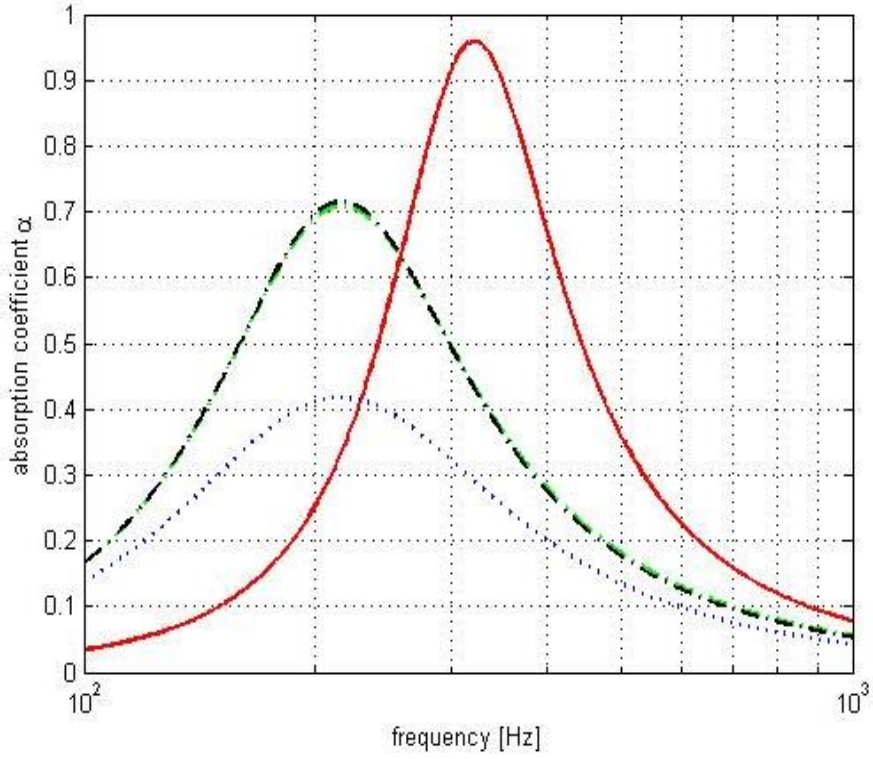

- Three tapered holes

SOURCE OF DISSIPATION

- **Plots of shear rate**

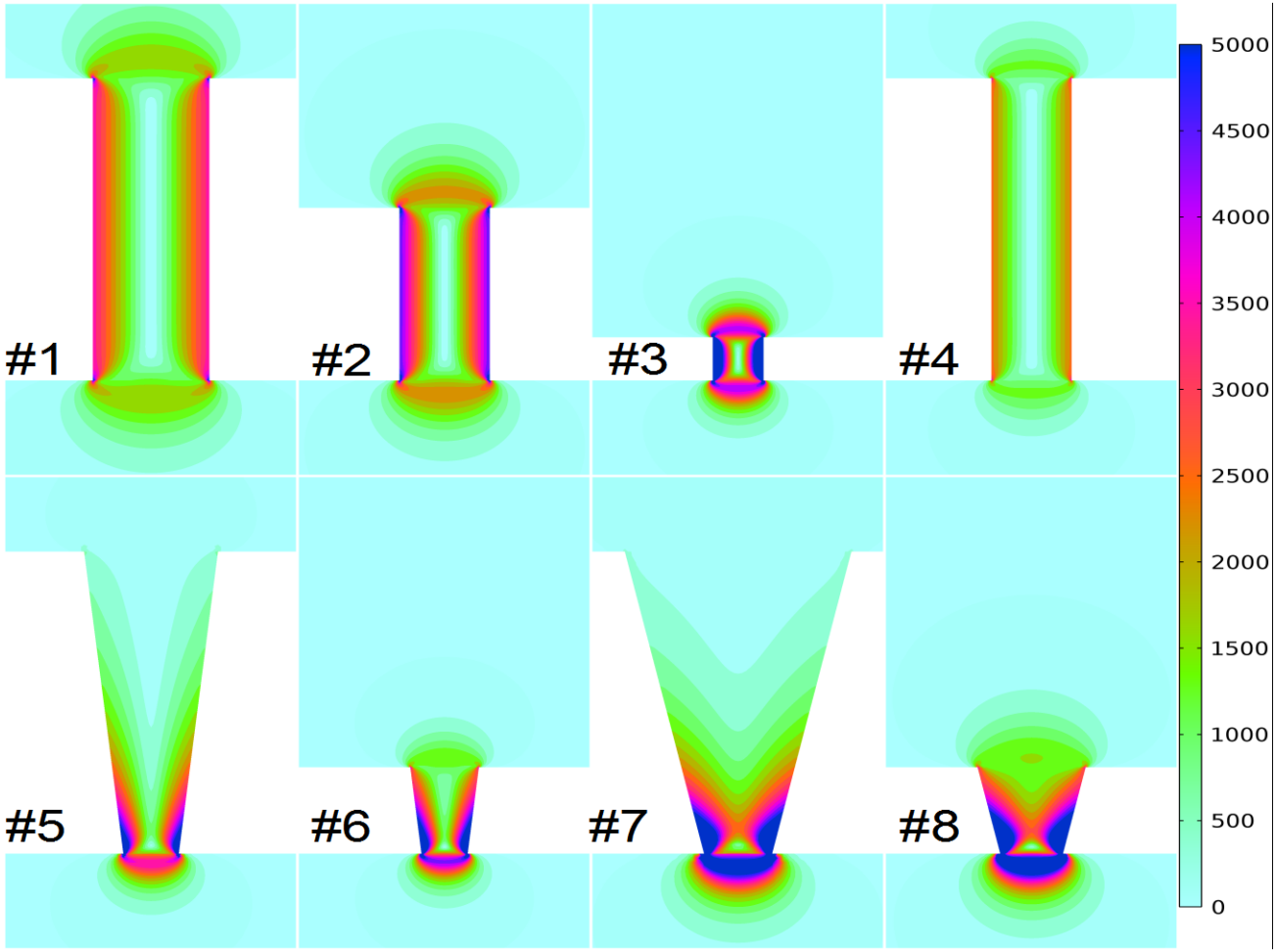

RIGID FILM – THERMAL LOSSES

- Thermal energy losses are proportional to the temperature gradient squared
  - Losses are concentrated over whole front surface, and only a little within the perforation
    (unlike Maa who modeled thermal losses occurring within the perforation)
  - Losses are asymmetric front-to-back *(acoustic wave is incident from below)*
  - Losses increase with the frequency *(Scale is 1/30th of viscous plots, so 1/900th the energy loss)*

$$\langle E_{loss} \rangle_k = \frac{k}{T} \left\langle |\nabla T|^2 \right\rangle$$

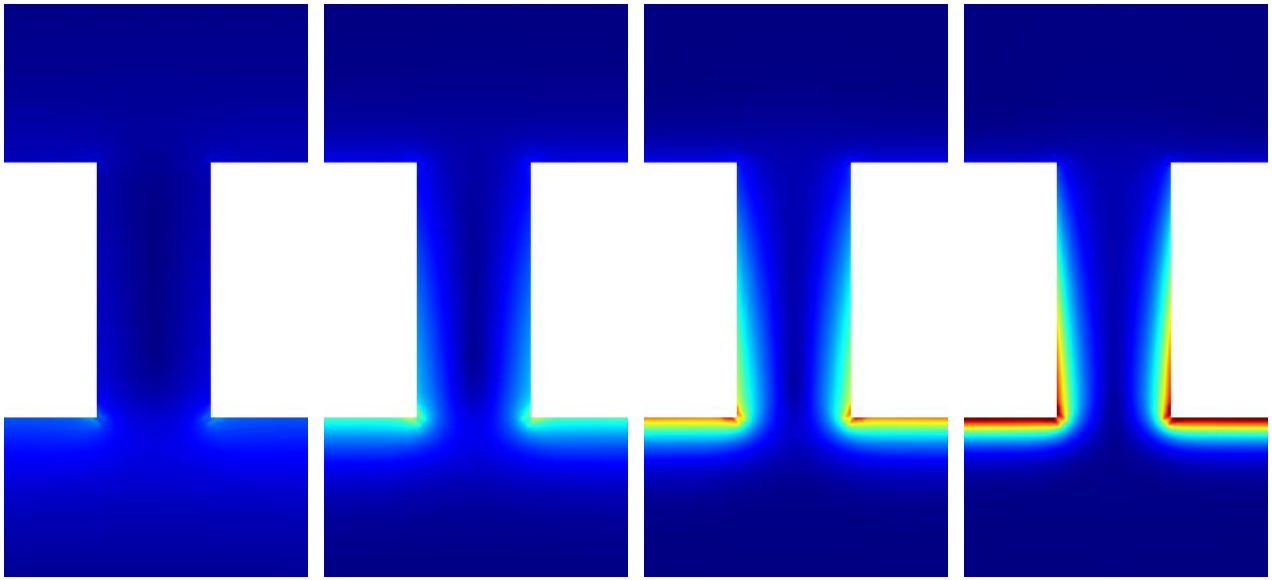

500 Hz 2,000 Hz 5,000 Hz 10,000 Hz

RIGID FILM – LOSSES COMPARED AND EFFECTIVE ABSORPTION

- Thermal losses are significantly smaller than viscous losses (< 5% up to 10 kHz)

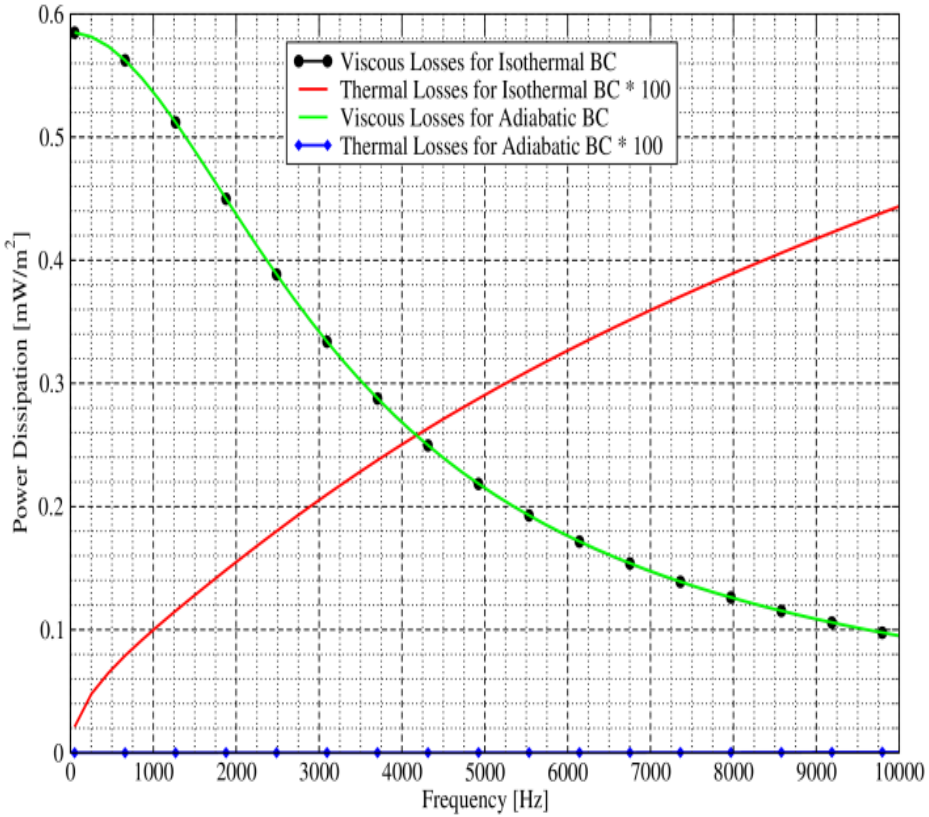

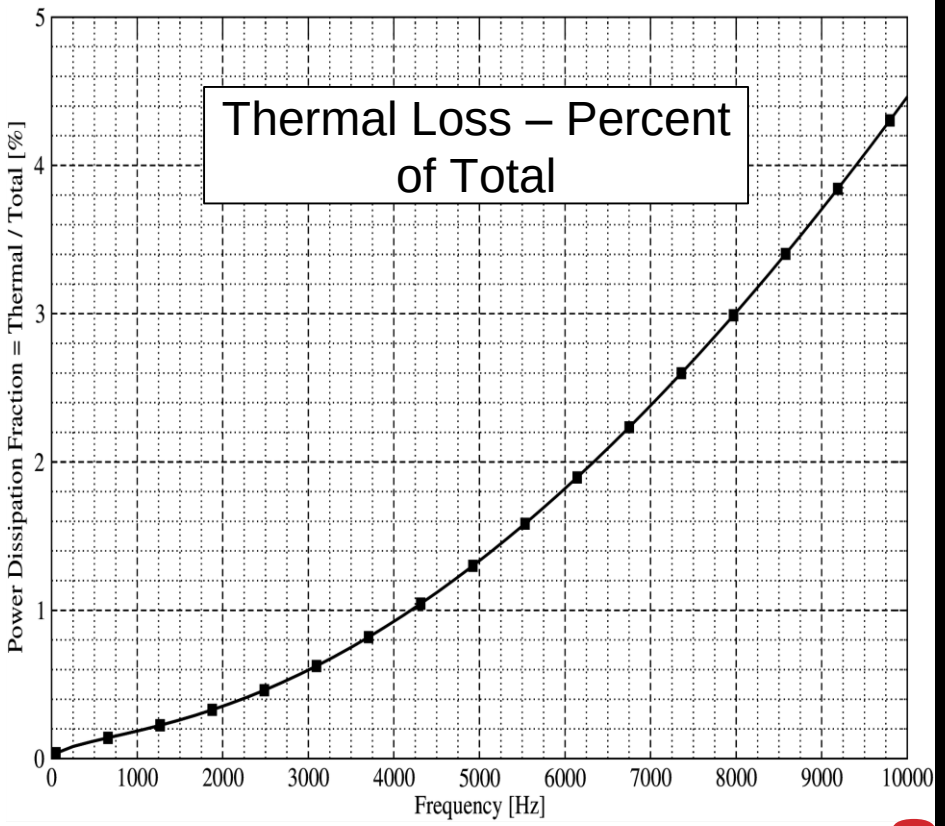

RIGID FILM – LOSSES COMPARED AND EFFECTIVE ABSORPTION

- Thermal boundary conditions (adiabatic vs. isothermal) are <u>not significant</u> for absorption
  - Infinite film in free space
  - Film in impedance tube with anechoic termination

$$\alpha = 1 - r - \tau$$

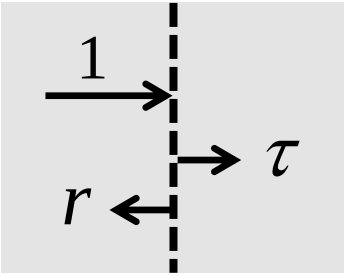

Absorption is the fraction of normally incident acoustic intensity not reflected or transmitted by the film.

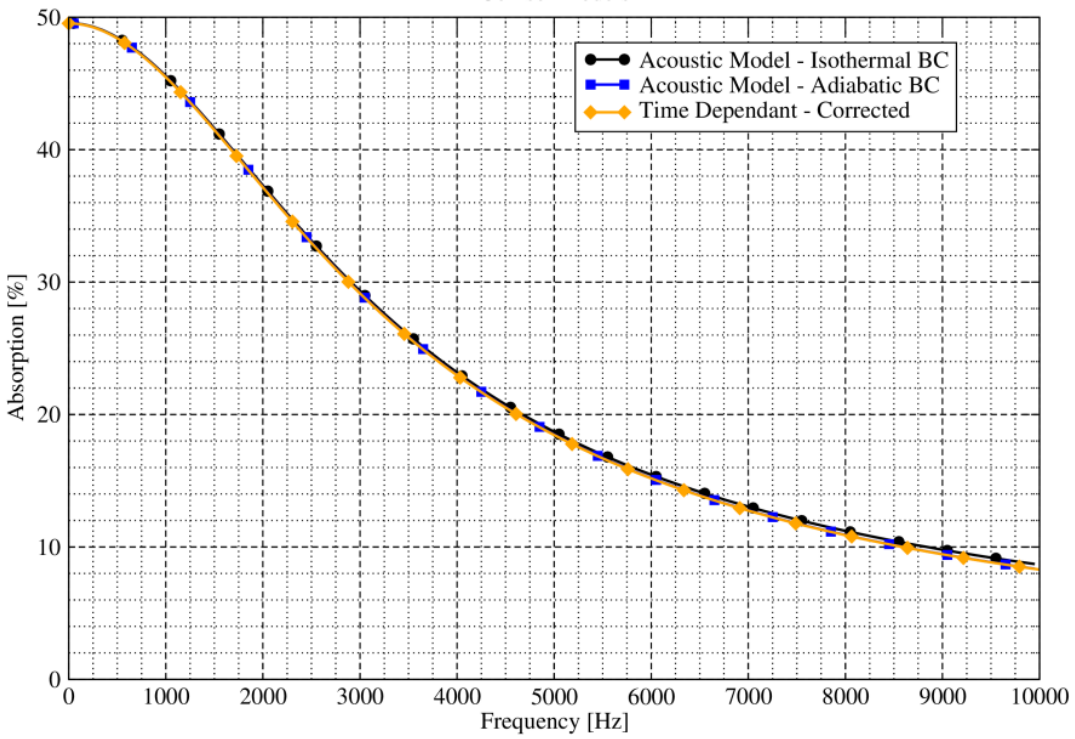

SUMMARY ON THERMAL LOSSES

- Thermal losses:
  - Increase with frequency
  - Occur over the full incident face of the film
    - Contributions from within the perforations are negligible
    - For moving films, losses occur on both sides of the film
      but the total thermal loss is almost identical to that of a rigid wall
  - Contribute to the acoustic resistance, but not the reactance
  - Are less than 5% of the total energy loss for practical films below 10 kHz
    - Have no significant effect on the predicted absorption

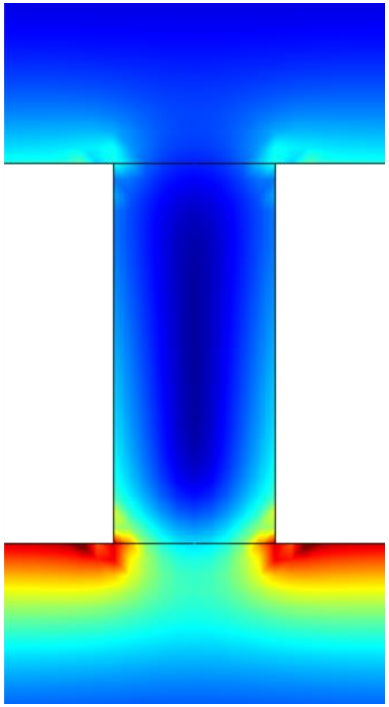

FILM FLEXIBILITY – EQUATIONS OF MOTION AND VELOCITY CONDITIONS

- **Flexible panel case**

Volume velocity continuity at x=0

$$\begin{cases} -\dfrac{1}{j\omega\rho_o}\dfrac{\partial p_I}{\partial x}\bigg|_{x=0} = (1-\Omega)\dfrac{\partial d_s}{\partial t} + \Omega\dfrac{\partial d_f}{\partial t} \\ -\dfrac{1}{j\omega\rho_o}\dfrac{\partial p_{II}}{\partial x}\bigg|_{x=0} = (1-\Omega)\dfrac{\partial d_s}{\partial t} + \Omega\dfrac{\partial d_f}{\partial t} \end{cases}$$

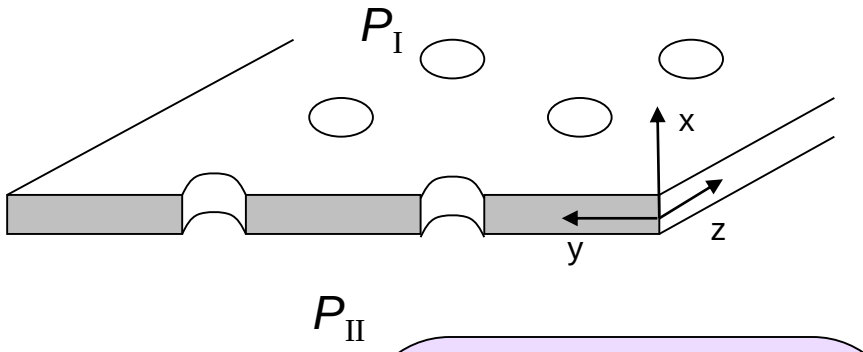

Force equilibrium at x=0

Solid
$$p_I - p_{II} + R_t\frac{\Omega^2}{1-\Omega}\frac{\partial(d_f - d_s)}{\partial t} = D\nabla^4 d_s - T\nabla^2 d_s + \rho_s\frac{\partial^2 d_s}{\partial t^2}$$

Fluid
$$p_I - p_{II} - R_t\Omega\frac{\partial(d_f - d_s)}{\partial t} = j\omega\rho_o h'\frac{\partial d_f}{\partial t}$$

- Panel motion important when m_s below 300 g/m^2

p_I: Pressure at source side

p_{II}: Pressure behind the panel

d_s: Displacement of solid part

d_f: Displacement of fluid part

ρ_s: Membrane mass per unit area

R_f: Flow resistance

D: Flexural stiffness

T: Tension

h': Effective thickness

Ω: Porosity

FILM FLEXIBILITY

- 3-dimensional model

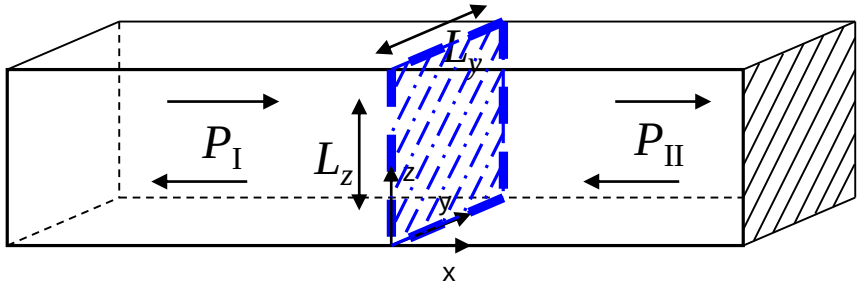

Only symmetric modes exist

Sound pressure in each region

$$P_I = e^{-jkx} + \sum_{m=0}^{\infty}\sum_{n=0}^{\infty} B_{mn}\cos(k_{2m}z)\cos(k_{2n}y)e^{jk_{x_{2m2n}}x}$$

$$P_{II} = \sum_{m=0}^{\infty}\sum_{n=0}^{\infty} C_{mn}\cos(k_{2m}z)\cos(k_{2n}y)\left(e^{-jk_{x2mn}x} + e^{jk_{x2mn}(x-2L)}\right)$$

$$k_{2m} = \frac{2m\pi}{L_z} \quad k_{2n} = \frac{2n\pi}{L_y} \quad (m,\ n=0,1,2,\ldots)$$

$$k_{x_{2m2n}} = \sqrt{k^2 - k_{2m}^2 - k_{2n}^2} \quad (k>k_{2n}+k_{2m})$$

$$= -j\sqrt{k^2 - k_{2m}^2 - k_{2n}^2} \quad (k<k_{2n}+k_{2m})$$

Displacement of membrane

for simply supported BC

Solid part $$d_s = \sum_{m=1}^{\infty}\sum_{n=1}^{\infty} A_{mn}\sin(k_{2m-1}z)\sin(k_{2n-1}y)$$

Fluid part $$d_f = \sum_{m=0}^{\infty}\sum_{n=0}^{\infty} F_{mn}\cos(k_{2m}z)\cos(k_{2n}y)$$

for clamped BC

Solid part $$d_s = \sum_{m=0}^{\infty}\sum_{n=0}^{\infty} A_{mn}\{\cos(k_{2m}z)-1\}\{\cos(k_{2n}y)-1\}$$

Fluid part $$d_f = \sum_{m=0}^{\infty}\sum_{n=0}^{\infty} F_{mn}\cos(k_{2m}z)\cos(k_{2n}y)$$

Taewook Yoo, J. Stuart Bolton, Jonathan H. Alexander and David F. Slama, “Absorption of finite-sized micro-perforated panels with finite flexural stiffness at normal incidence,” *Proceedings of NOISE-CON 2008*, Dearborn, Michigan, July 28-31, 2008.

MEASUREMENT OF PLEXIGLASS SAMPLES

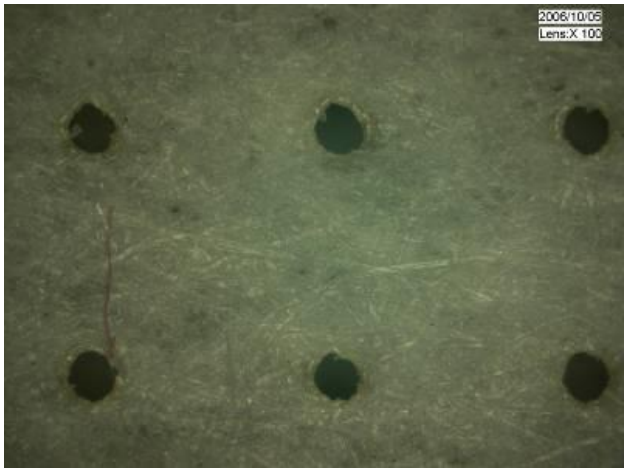

Sample 1 (x100)

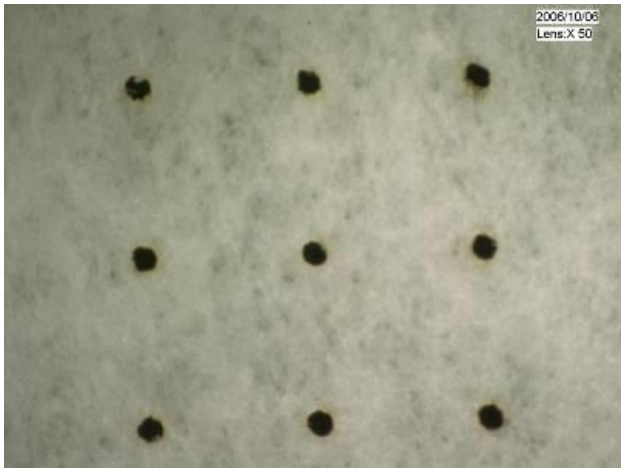

Sample 2 (x50)

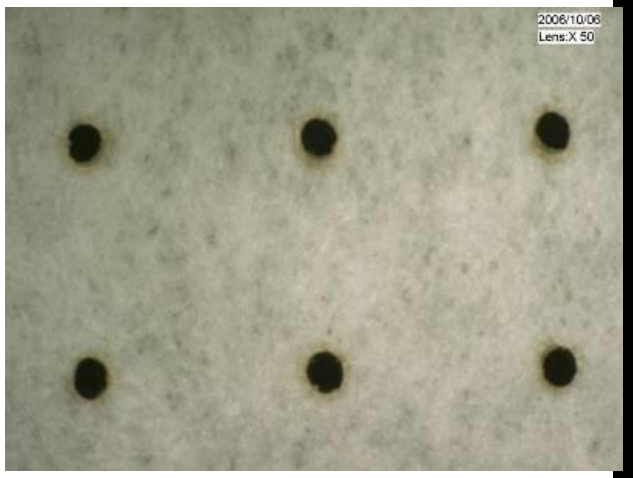

Sample 3 (x50)

	d (nominal) [mm]	t [mm]	ρ_s [kg/m^2]	N
Sample 1	0.254	1.588	1.584	722500
Sample 2	0.2667	1.588	1.627	291600
Sample 3	0.4064	1.588	1.631	160000

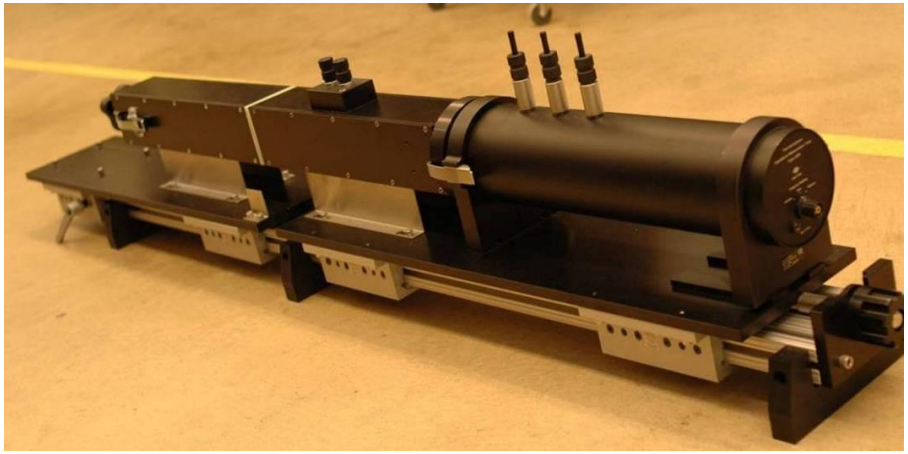

COMPARISON BETWEEN PREDICTIONS AND MEASUREMENTS

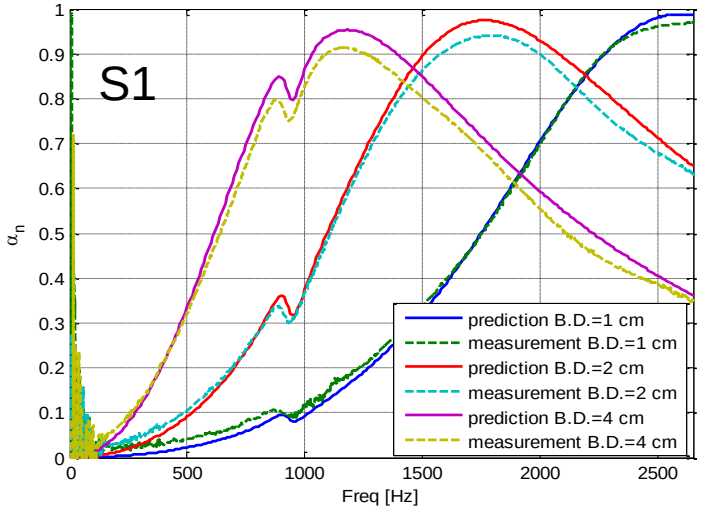

	d (nominal) [mm]	*d* (adjusted) [mm]	*t* [mm]	*D* / loss factor [N·m²]	*T* [N]	ρ_s [kg/m²]	*N*
S1	0.254	0.305	1.588	0.7/ 0.07	0	1.584	72250
S2	0.2667	0.35	1.588	0.7/ 0.07	0	1.627	29160
S3	0.4064	0.45	1.588	0.7/ 0.07	0	1.631	16000

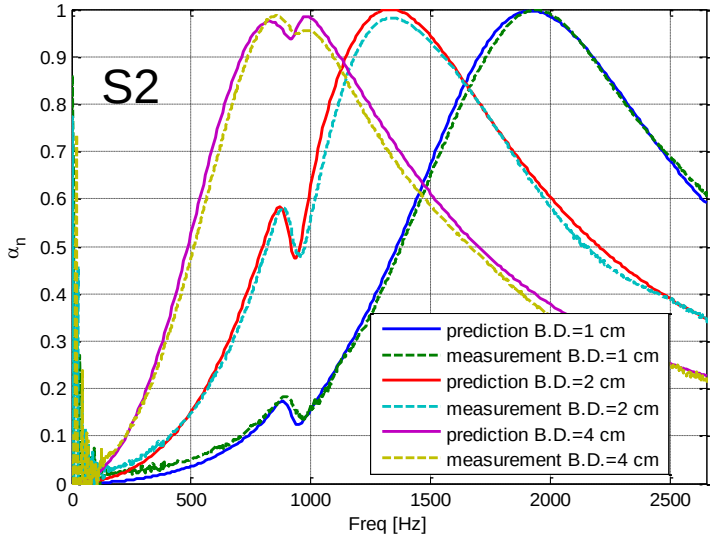

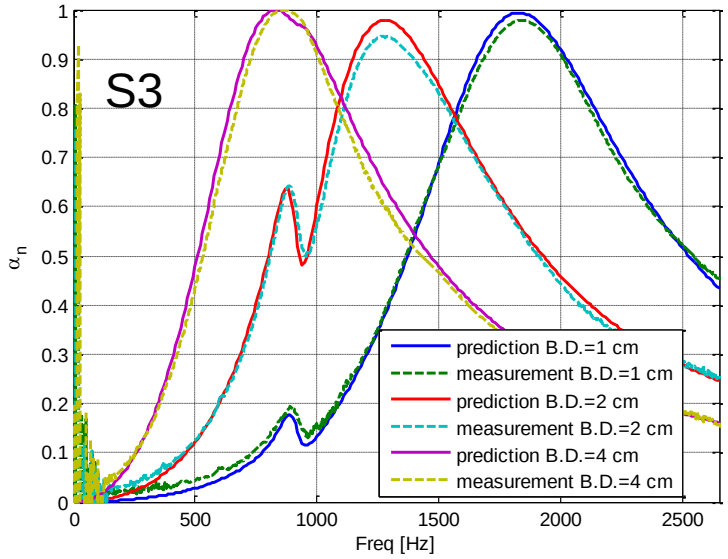

FLEXURAL STIFFNESS EFFECT

- **Significant when basis weight < 300 g/m²**

d [mm]	*t* [mm]	*D* [N·m²]	loss factor in *D*	*T* [N]	Mass/area [kg/m²]	*N*	Size [mm]
0.45	1.588	1, 0.6, 0.4, 0.3, 0.2, 0.1, 0.01, 0.0001	0.05	0	0.1631	160000	63.5 x 63.5

- Depending on the flexural stiffness, the absorption performance can be enhanced with a proper loss factor

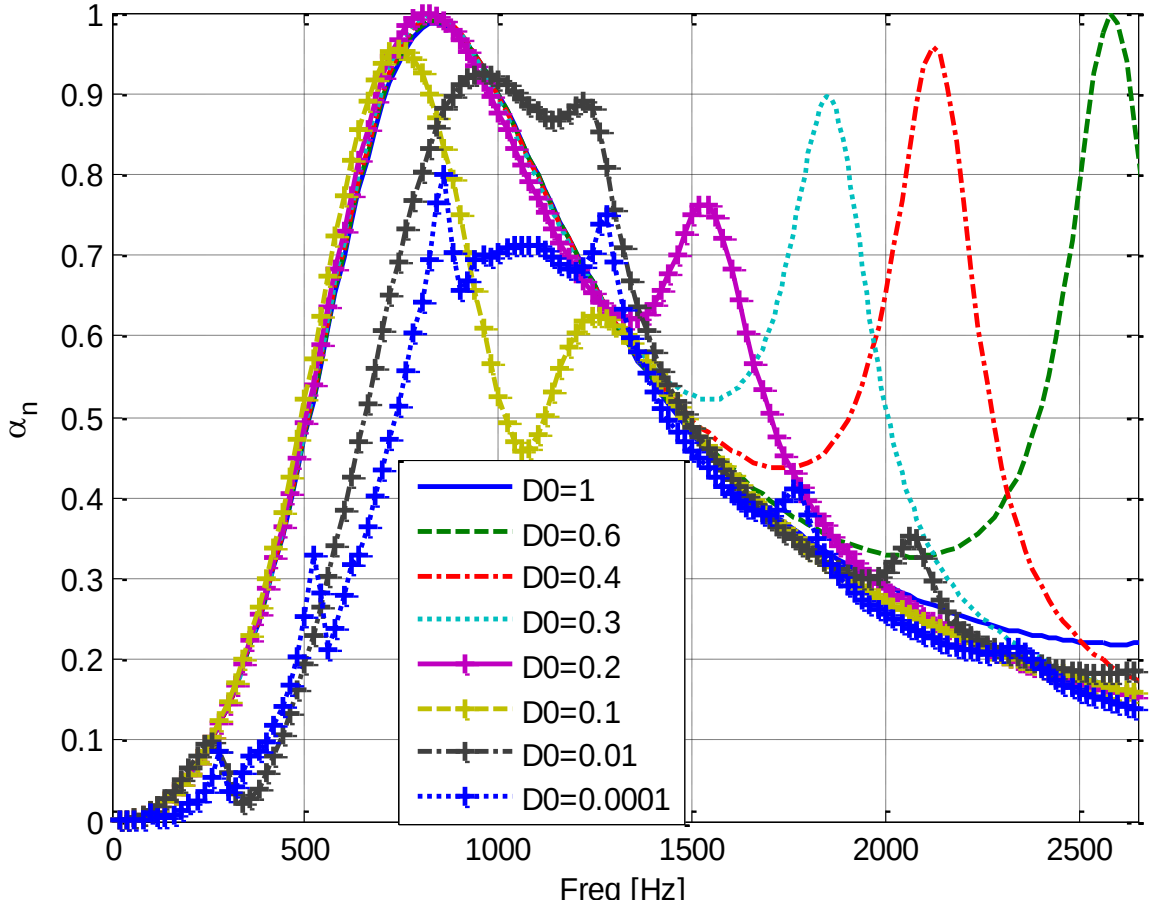

LIMP PERFORATED FILM – IMPEDANCE

- **Mass Law impedance for limp impervious sheet added in parallel to the impedance of a rigid perforated plate predicts response very well (markers)**

$$Z_{Film} = \frac{1}{\frac{1}{Z_{Rigid}} + \frac{1}{Z_{Sheet}}} = \frac{j\omega m \cdot Z_{Rigid}}{Z_{Rigid} + j\omega m}$$

- ➢Resistance drops as mass decreases
- ➢Reactance changes in non-intuitive manner
- ➢Low-frequency has an increase of reactance with mass
- ➢High-frequency approaches rigid results more directly

Film Resistance – FSI models compared to formula

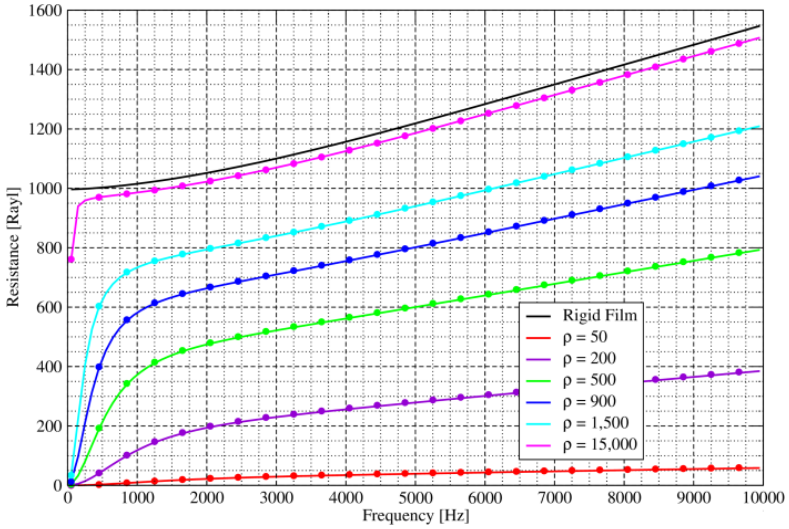

Film Reactance – FSI models compared to formula

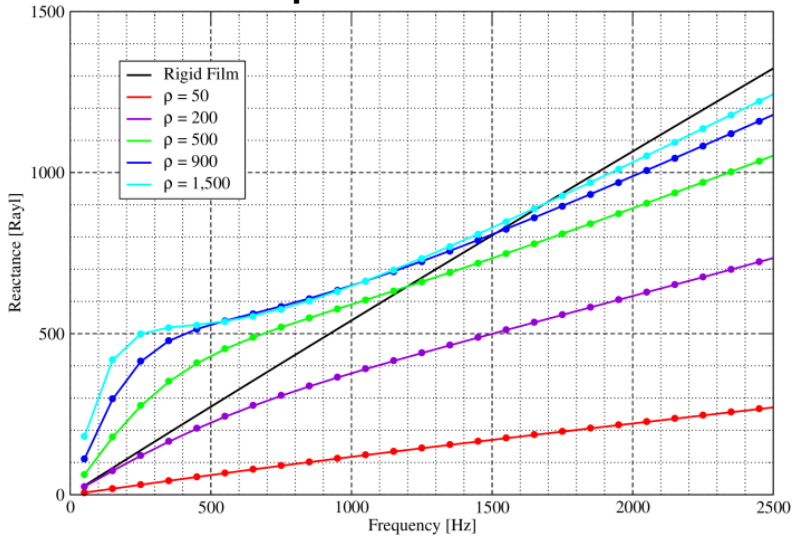

CONCLUSIONS – CFD MODELING

- Computational modeling of MPP's has proven to be a powerful tool
- Has allowed identification of the correct origin of the resistive end correction
- Accurate calculation of transfer impedance of MPP's with arbitrarily shaped holes
- For thermally conducting materials, thermal losses occur on surface of MPP (not within holes), but contribution to energy dissipation generally negligible
- Solid – phase motion influences MPP transfer impedance, but large disparity between solid and fluid velocities allows transfer impedance to be calculated by parallel addition of rigid MPP and flexible impermeable film

DUCT LINING APPLICATION

- **HVAC systems**

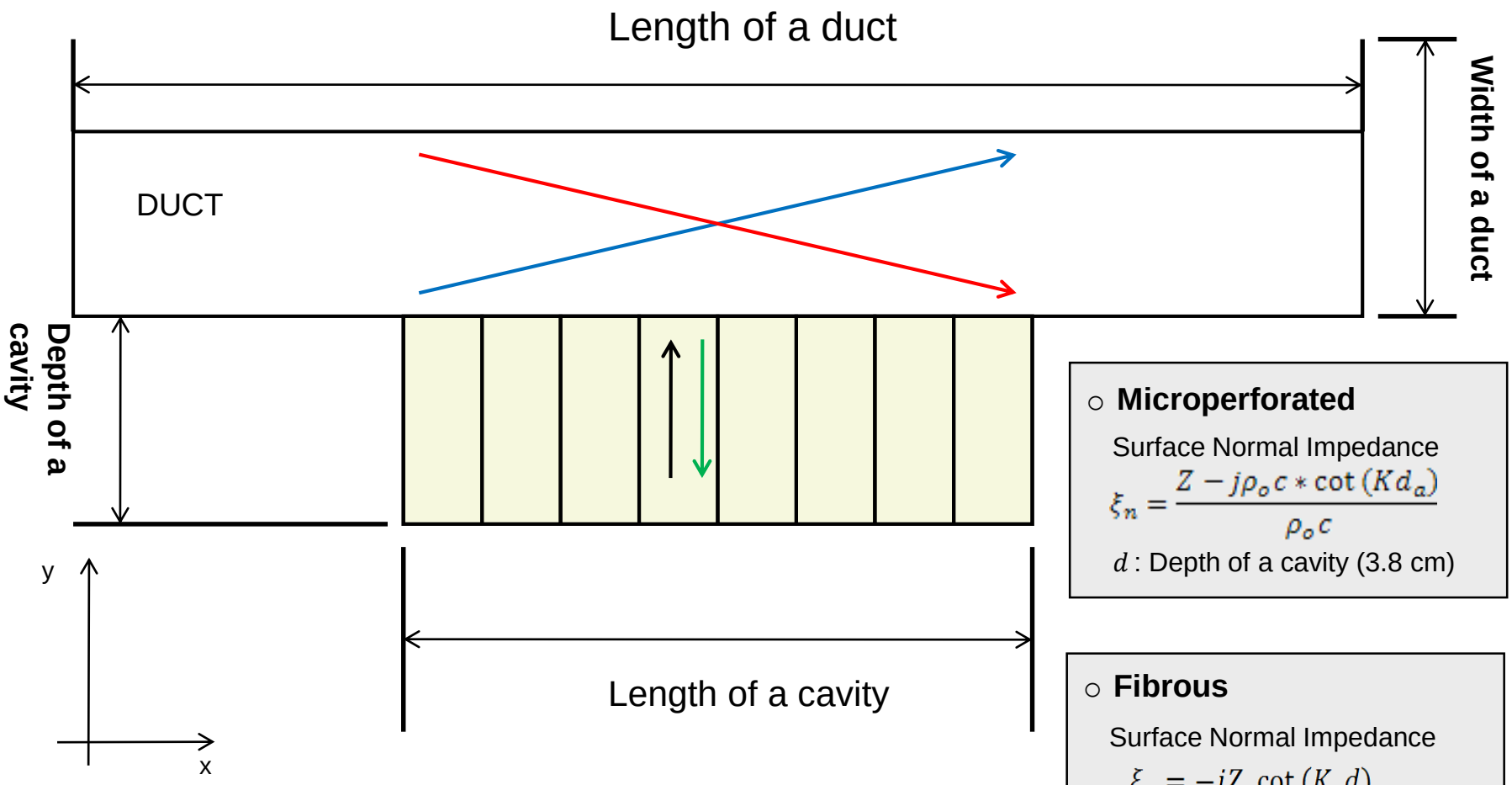

- **Microperforated**

  Surface Normal Impedance

$$\xi_n = \frac{Z - j\rho_o c * \cot(Kd_a)}{\rho_o c}$$

  d : Depth of a cavity (3.8 cm)

- **Fibrous**

  Surface Normal Impedance

$$\xi_n = -jZ_o \cot(K_p d)$$

  d : Depth of a cavity (3.8 cm)

Herrick Labs, Purdue University

FINITE ELEMENT MODEL APPROACHES

- **Modeling microperforate as a rigid porous material**
  - Attala and Sgard model is explicitly used to model

Flow resistivity $\varphi = \frac{8\eta}{\sigma r^2}$ Tortuosity $\alpha_\infty = 1 + \frac{\varepsilon_e}{t}$

Correction length $\varepsilon_e = 0.48\sqrt{\pi r^2}(1 - 1.4\sqrt{\varphi})$

Surface impedance with a finite-depth air cavity

$$Z_A = \left(\frac{2t}{r} + 4\right)\frac{R_s}{\varphi} + \frac{1}{\varphi}(2\varepsilon_e + d)j\omega\rho_o - j\rho_o c_o \cot(k_o L)$$

$$R_s = \frac{1}{2}\sqrt{2\eta\omega\rho_o}$$

Viscous and thermal characteristic lengths $\Lambda = \Lambda' = r$

η : dynamic viscosity σ : porosity r : radius t : thickness

FINITE ELEMENT MODEL APPROACHES

- **Local and extended reaction treatments for fibrous material**

Local reaction case

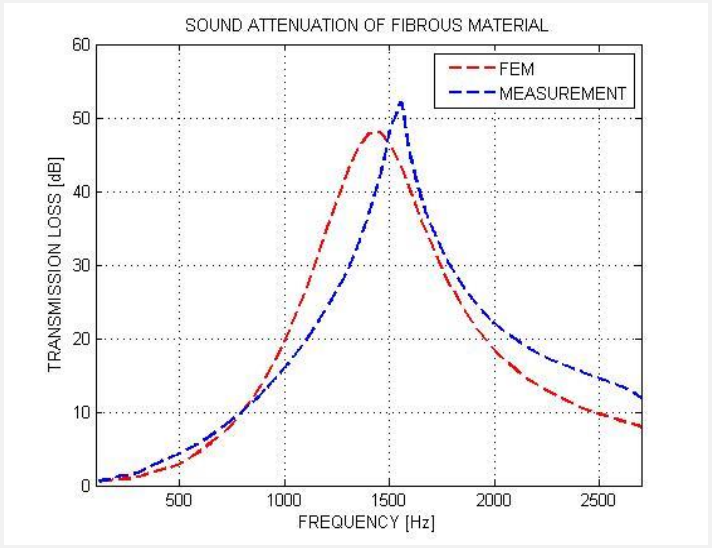

Extended reaction case

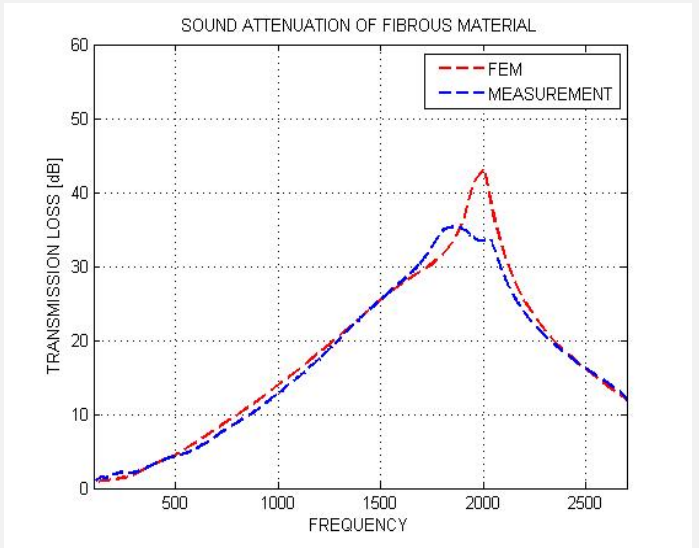

FINITE ELEMENT MODEL APPROACHES

- **Local and extended reaction treatments for microperforated material**

Local reaction case

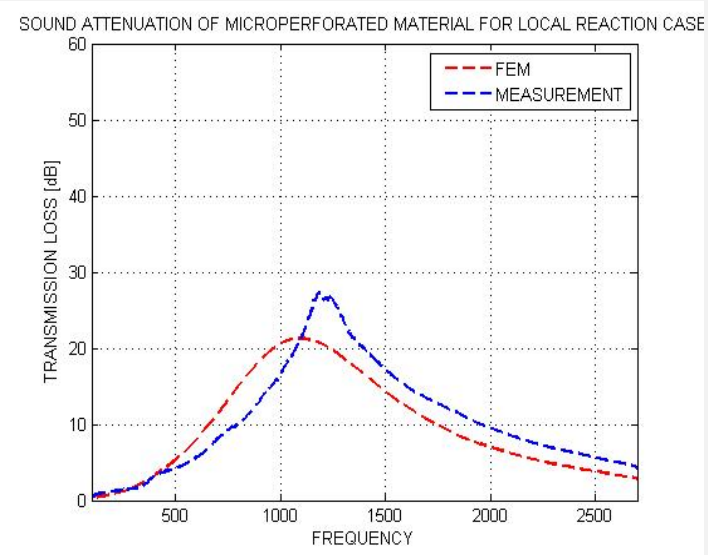

Extended reaction case

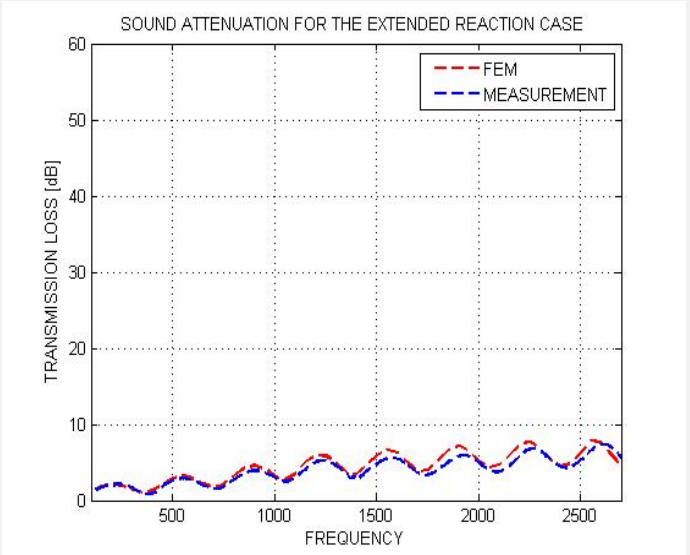

MATCHING FIBROUS PERFORMANCE

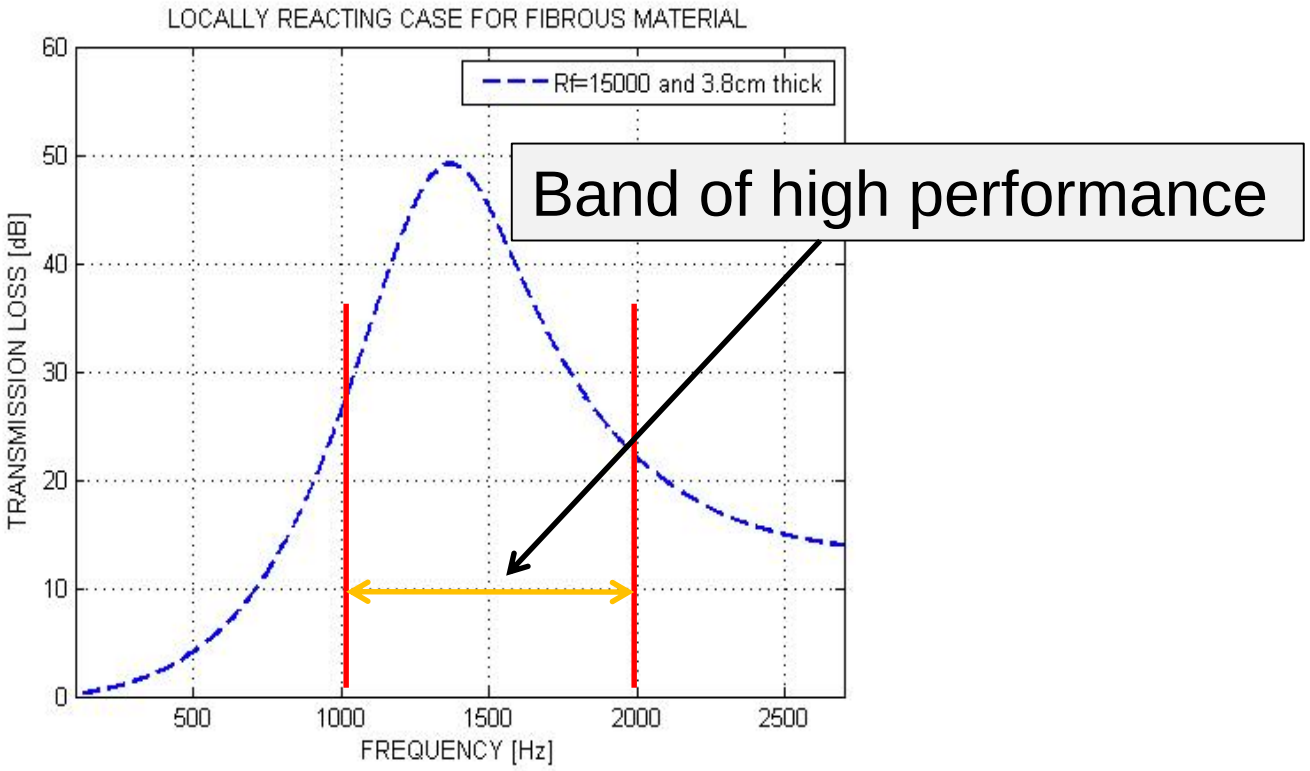

- **To match TL performance, create microperforated treatment having same surface normal impedance as fibrous layer in high performance band**

COMPARISONS

- **Microperforated material matching acoustical performance of fibrous material**

NORMALIZED IMPEDANCE

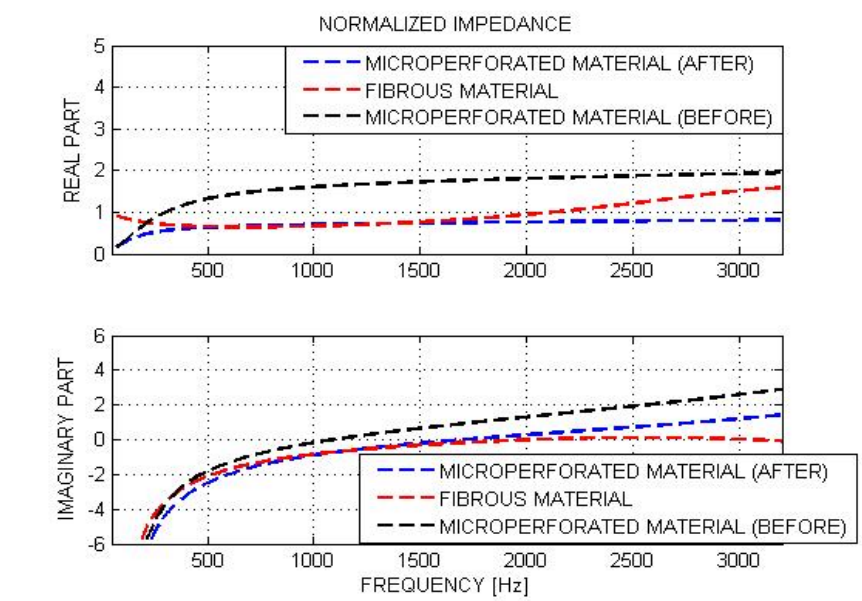

• 3.8 cm air backing depth for microperforated material

•3.8 cm thick fibrous material

• Least square error method is applied to match the both real and imaginary part of fibrous material by adjusting the parameters of microperforated material.

COMPARISONS

- **Transmission loss of duct linings**

Local reaction treatment
(Analytical approach)

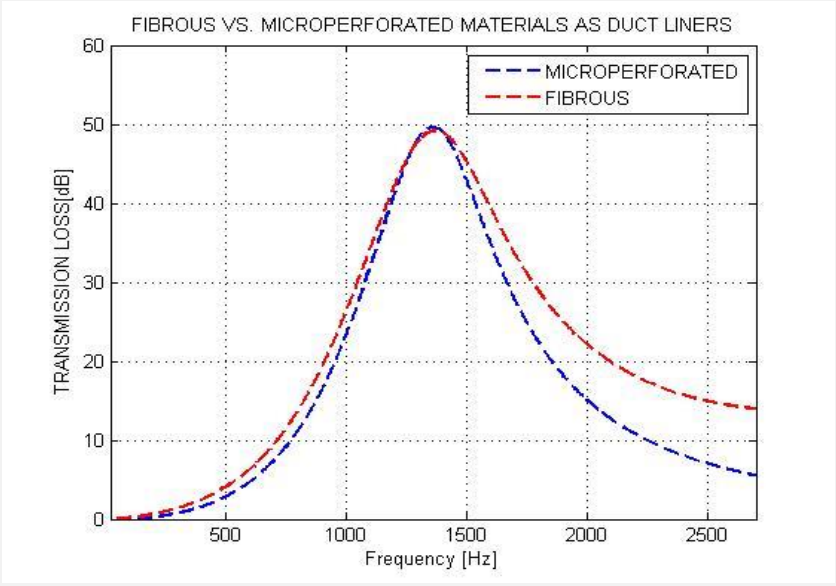

Local reaction treatment
(Finite element approach)

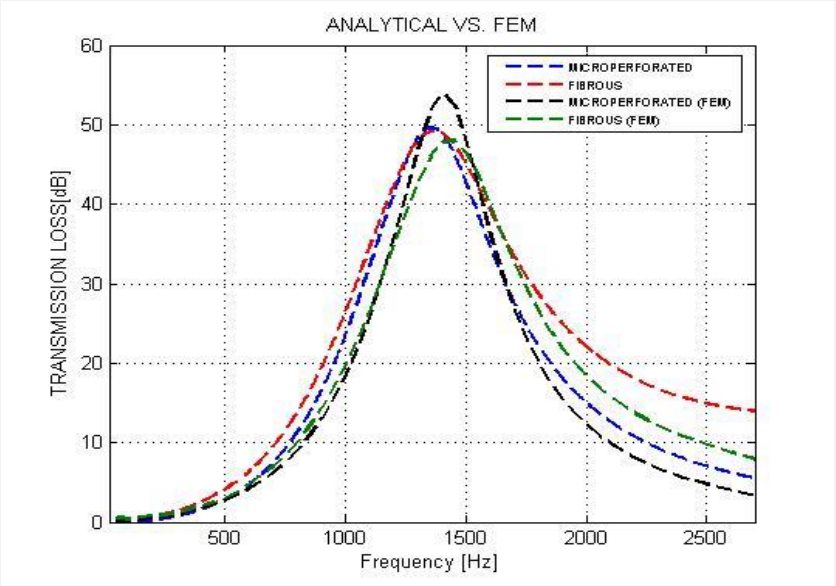

CONCLUSIONS

- **MPP's first new noise control material in decades**
- **Good acoustic performance in a number of different applications with many attractive functional attributes**
- **Theoretical modeling is relatively simple but there are a number of practical complications**
  - Origin and magnitude of resistive end correction
  - Hole geometry
  - Panel flexibility
- **Micro-scale CFD and finite elements offer a powerful tool for determining transfer impedances of realistic treatments**
- **MPP's can be modeled at a macro scale as poroelastic media**

PURDUE MPP REFERENCES

- Seungkyu Lee and J. Stuart Bolton, "Design of multi-chamber silencers with microperforated elements," *Noise Control Engineering Journal*, Vol. 64(4), 532-543, 2016.
- Seungkyu Lee and J. Stuart Bolton, "Testing of fans with microperforated housings," *Noise Control Engineering Journal*, Vol. 64(4), 511-521, 2016.
- T. Herdtle, J.S. Bolton, N.N. Kim, J.H. Alexander and R.W. Gerdes, "Transfer impedance of microperforated materials with tapered holes," Journal of the Acoustical Society of America, Vol. 134(6), Pt. 2, Special Issue, 4752-4762, 2013. DOI: 10.1121/1.4824968.
- J. S. Bolton and N. Kim, "Use of CFD to calculate the dynamic resistive end correction for microperforated materials," Acoustics Australia, Vol. 38, issue 3, 134-139, 2010.
- Seung-kyu Lee and J. Stuart Bolton, "The application of microperforated material to control axial fan noise," Proceedings of FAN2015: International Conference on Fan Noise, Technology and Numerical Methods, 13 pages, Lyon, France, April 2015
- Seungkyu Lee and J. Stuart Bolton, "Design of an acoustic silencer with microperforated elements considering flow effects," Proceedings of InterNoise 2015, 15 pages, San Francisco CA, 2015.
- Seungkyu Lee and J. Stuart Bolton, "Study of an axial fan combined with a microperforated duct," Proceedings of InterNoise 2015, 13 pages, San Francisco CA, 2015.
- Nicholas N. Kim and J. Stuart Bolton, "Microperforated films as duct liners," Proceedings of InterNoise 2015, 10 pages, San Francisco CA, 2015.
- Seung-kyu Lee, J. Stuart Bolton and Paul A. Martinson, "Design of multi-chamber silencers with microperforated elements," Proceedings of Noise-Con 2014, Fort Lauderdale FL, 12 pages, 2014.
- Thomas Herdtle and J. Stuart Bolton, "Effect of Thermal Losses and Fluid-Structure Interaction on the Transfer Impedance of Microperforated Films," Proceedings of Noise-Con 2014, Fort Lauderdale FL, 12 pages, 2014.

Go to: http://docs.lib.purdue.edu/herrick/ for related presentations (search for: Herrick epubs)

PURDUE MPP REFERENCES

- Nicholas N. Kim and J. Stuart Bolton, "Optimization of multi-layer microperforated systems for absorption and transmission loss," Proceedings of Noise-Con 2014, Fort Lauderdale FL, 8 pages, 2014.
- Seung-kyu Lee and J. Stuart Bolton, "Testing of fans with microperforated housings," Proceedings of Noise-Con 2013, Denver CO, 9 pages, 2013.
- Arun Viswanathan and J. Stuart Bolton, "Study of the effect of grazing flow on the performance of microperforated and perforated panels," Proceedings of Noise-Con 2013, Denver CO, 8 pages, 2013.
- Ryan A. Schultz, J. Stuart Bolton, Jonathan H. Alexander, Stephanie B. Castiglione, Tom P. Hanschen and Ed Bronikowski, "Improving the visitor experience – a noise study and treatment design for the Smithsonian National Zoological Park's Great Ape House," Proceedings of INTER-NOISE 2012, 8 pages, 2012.
- Nicholas N. Kim and J. Stuart Bolton, "CFD modeling of tapered hole microperforated panels," Proceedings of INTER-NOISE 2012, 11 pages, 2012.
- H. Shin and J. Stuart Bolton, "Microperforated materials as duct liners: Local reaction versus extended reaction," Proceedings of NOISE-CON 2011, 748-760, 2011.
- N. Kim and J.S. Bolton, "Use of CFD to calculate the transfer impedance of microperforated materials having round-edged holes," Proceedings of NOISE-CON 2011, 774-784, 2011.
- T. Herdtle, R. Gerdes, J.H. Alexander and J.S. Bolton, "Transfer impedance of microperforated materials with tapered holes," Proceedings of INTER-NOISE 2011, 4448-4455, 2011.
- J.S. Bolton and N. Kim, "Use of CFD to calculate the dynamic resistive end correction for microperforated materials," Proceedings of the 20th International Congress on Acoustics, 8 pages, Sydney, Australia, August 2010.
- J.S. Bolton and N. Kim, "Use of CFD to calculate the performance of microperforated materials," Proceedings of INTER-NOISE 2010, 8 pages, Lisbon, Portugal, June 2010.

PURDUE MPP REFERENCES

- H. Shin and J.S. Bolton, “The use of microperforated materials as duct liners,” Proceedings of INTER-NOISE 2010, 9 pages, Lisbon, Portugal, June 2010.
- K. Hou and J.S. Bolton, “Finite element models for micro-perforated materials,” Proceedings of INTER-NOISE 2009, 9 pages, Ottawa, Canada, August 2009.
- K. Hou and J.S. Bolton, “Validation of micro-perforated panel models,” Proceedings of INTER-NOISE 2008, 7 pages, Shanghai, China, October 2008.
- T. Yoo, J.S. Bolton, J.H. Alexander and D.F. Slama, “Absorption from finite-size microperforated panels at arbitrary incidence angles,” Proceedings of the 15th International Congress on Sound and Vibration, Daejeon, Korea, July 6-10, 2008.
- Taewook Yoo, J. Stuart Bolton, Jonathan H. Alexander and David F. Slama, “Absorption of finite-sized micro-perforated panels with finite flexural stiffness at normal incidence,” Proceedings of NOISE-CON 2008, Dearborn, Michigan, July 28-31, 2008.
- Niranjan R. Londhe, J. Stuart Bolton, Taewook Yoo, Jonathan H. Alexander, and David F. Slama, “Random incidence sound absorption coefficient of micro-perforated absorbers,” Proceedings of NOISE-CON 2007, 1643-1653, Reno, Nevada, October 2007.
- Taewook Yoo, J. Stuart Bolton, Jonathan H. Alexander, and David F. Slama, “An improved model for micro-perforated absorbers,” Proceedings of NOISE-CON 2007, 1654-1661, Reno, Nevada, October 2007.
- Jinho Song and J. Stuart Bolton, “Acoustical modeling of tensioned, permeable membranes,” Proceedings of NOISE-CON 2003, paper nc03_211, 6 pages, Cleveland, Ohio, June 2003.
- Jinho Song and J. Stuart Bolton, “Sound absorption characteristics of membrane-based sound absorbers,” Proceedings of INTER-NOISE 2003, paper N286, 8 pages, Seogwipo, South Korea, August 2003.
- Jinho Song and J. Stuart Bolton, “Modeling of membrane sound absorbers,” Proceedings of INTER-NOISE 2002, paper N574, 6 pages, Dearborn, Michigan, August 2002.

RECENT MPP RESEARCHERS

Mats Abom *KTH Stockholm*

Ines Lopez Arteaga *KTH Stockholm*

David Herrin *University of Kentucky*

Cedric Maury *LMA / CNRS Marseille*

Christian Nocke *Oldenburg*

Kimihiro Sakagami *Kobe University*

Jing Tian *Institute of Acoustics, Chinese Academy of Science*

Masahiro Toyoda *Kansai University*

ACKNOWLEDGEMENTS

- **3M Company**
  - Jon Alexander
  - Ron Gerdes
  - Tom Hanschen
  - Thomas Herdtle
  - Dave Slama
- **Current or Previous Students**
  - Kang Hou *Apple*
  - Nicholas Kim *Purdue*
  - Seungkyu Lee *3M*
  - Ryan Schultz *Sandia National Labs*
  - Hyunjun Shin *Purdue/Tesla*
  - Jinho Song *Otis Elevators*
  - Arun Viswanathan *Simulia*
  - Yutong Xue *Purdue*
  - Taewook Yoo *3M*